Quantifying Protein Synthesis and Degradation in Arabidopsis by Dynamic $^{13}CO_2$ Labeling and Analysis of Enrichment in Individual Amino Acids in Their Free Pools and in Protein[1][OPEN]

Hirofumi Ishihara, Toshihiro Obata, Ronan Sulpice[2], Alisdair R. Fernie, and Mark Stitt*

Max Planck Institute of Molecular Plant Physiology, 14476 Potsdam-Golm, Germany

ORCID IDs: 0000-0002-7658-0473 (H.I.); 0000-0001-8931-7722 (T.O.); 0000-0002-6113-9570 (R.S.).

Protein synthesis and degradation represent substantial costs during plant growth. To obtain a quantitative measure of the rate of protein synthesis and degradation, we supplied $^{13}CO_2$ to intact Arabidopsis (*Arabidopsis thaliana*) Columbia-0 plants and analyzed enrichment in free amino acids and in amino acid residues in protein during a 24-h pulse and 4-d chase. While many free amino acids labeled slowly and incompletely, alanine showed a rapid rise in enrichment in the pulse and a decrease in the chase. Enrichment in free alanine was used to correct enrichment in alanine residues in protein and calculate the rate of protein synthesis. The latter was compared with the relative growth rate to estimate the rate of protein degradation. The relative growth rate was estimated from sequential determination of fresh weight, sequential images of rosette area, and labeling of glucose in the cell wall. In an 8-h photoperiod, protein synthesis and cell wall synthesis were 3-fold faster in the day than at night, protein degradation was slow (3%–4% d^{-1}), and flux to growth and degradation resulted in a protein half-life of 3.5 d. In the starchless *phosphoglucomutase* mutant at night, protein synthesis was further decreased and protein degradation increased, while cell wall synthesis was totally inhibited, quantitatively accounting for the inhibition of growth in this mutant. We also investigated the rates of protein synthesis and degradation during leaf development, during growth at high temperature, and compared synthesis rates of Rubisco large and small subunits of in the light and dark.

Protein synthesis accounts for a significant part of the energy required for plant growth (Penning de Vries et al., 1974; Penning de Vries, 1975; Amthor, 2000). The rate of protein synthesis can be qualitatively assessed by investigating the proportion of ribosomes loaded into polysomes (Bailey-Serres, 1999; Beilharz and Preiss, 2004). Polysome loading decreases in various stress treatments, including water deficit (Hsiao, 1970; Kawaguchi et al., 2003, 2004) and hypoxia (Branco-Price et al., 2005, 2008). In nonstressed plants in a light/dark cycle, polysome loading is high in the light and decreases in the dark (Piques et al., 2009; Pal et al., 2013). Polysome loading is increased by sugar addition to cell cultures (Nicolaï et al., 2006) and is closely correlated with Suc levels during diurnal cycles in Arabidopsis (*Arabidopsis thaliana*) rosettes (Pal et al., 2013). Information about polysome loading and ribosome abundance has been used to model the rate of protein synthesis in Arabidopsis rosettes (Piques et al., 2009; Pal et al., 2013). This approach indicated that the rate of protein synthesis is higher in the daytime than at night, when it is constrained by the rate of starch degradation and the resulting availability of carbon (C) and energy. It also indicated that the global rate of protein synthesis is only slightly higher than that needed for growth, indicating that there is only a low rate of protein degradation.

Protein degradation is required to repair damaged proteins, to adjust the protein complement to environmental conditions, and to remobilize and recycle amino acids (Huffaker and Peterson, 1974; Nelson et al., 2014b). Protein degradation is thought to make a major impact on growth efficiency (Amthor, 2000). It has been estimated that protein degradation accounts for 20% to 30% of the ATP produced by root respiration (Scheurwater et al., 2000). Protein degradation is accelerated in low nitrogen (Lattanzi et al., 2005; Lehmeier et al., 2013) and by shading (Pons et al., 1993; Scheurwater et al., 2000); this may promote nitrogen remobilization to young leaves in more favorable light conditions. Protein degradation is accelerated under C starvation to provide an alternative source of C for respiration (Brouquisse et al., 1991; Araújo et al., 2011; Izumi et al., 2013; Pilkington et al., 2015). Protein degradation may also increase

[1] This work was supported by the Max Planck Society and the European Union (collaborative project TiMet under contract no. 245143).

[2] Present address: National University of Galway, Plant Systems Biology Laboratory, Plant and AgriBiosciences Research Centre, Botany and Plant Science, Aras de Brun, University Road, Galway, Republic of Ireland.

* Address correspondence to mstitt@mpimp-golm.mpg.de.

The author responsible for distribution of materials integral to the findings presented in this article in accordance with the policy described in the Instructions for Authors (www.plantphysiol.org) is: Mark Stitt (mstitt@mpimp-golm.mpg.de).

[OPEN] Articles can be viewed without a subscription.

www.plantphysiol.org/cgi/doi/10.1104/pp.15.00209

under other stresses, including high temperature in wheat (*Triticum aestivum*) roots (Ferguson et al., 1990) and osmotic stress in barley (*Hordeum vulgare*) leaves (Dungey and Davies, 1982). It may also change during leaf development, with various studies indicating that degradation is higher in expanding than in fully grown leaves (Schaefer et al., 1981; Barneix et al., 1988) and also increases in old leaves (Dungey and Davies, 1982; Bouma et al., 1994).

Protein half-life depends on the rate of degradation and on the rate at which preexisting protein is diluted by growth. Global protein half-life was estimated to be 4 to 8 d in grass roots (Scheurwater et al., 2000). A similar protein half-life was predicted by modeling in Arabidopsis rosettes (Piques et al., 2009) and by experimental studies of 508 individual proteins in barley leaves (Nelson et al., 2014a).

The rate of protein synthesis is usually measured by supplying a pulse of a labeled precursor, often followed by a chase in the absence of label, and monitoring the temporal kinetics of label incorporation and depletion (Huffaker and Peterson, 1974; Nelson et al., 2014b). While radioisotopes were used in the past, stable isotopes are easier to detect and quantify in specific compounds. Labeling experiments should meet several criteria. First, the labeled precursor must be supplied without surgical or other disturbance of the plant, as this may alter the rates of protein synthesis and degradation. Second, the supplied labeled precursor should not alter internal metabolite pools or fluxes. Third, movement of label per se does not provide information about flux. This requires information about the extent to which the incoming label is diluted by internal pools. Fourth, accurate measurements of the rate of growth are required to assess how much of the protein synthesis represents flux to growth and how much represents protein turnover (viz., the replacement of degraded proteins). Many studies in the past did not meet all these criteria; in particular, they rarely measured enrichment in the free amino acid precursor pools.

Labeled amino acids have been widely used in microbes to study protein synthesis. To decrease dilution by internal pools, an amino acid is used that the microbe cannot synthesize. Similar approaches have been used in human cell cultures (Ong et al., 2002; Ong and Mann, 2006). While labeled amino acids have also been used in algae and plants, the resulting data are usually qualitative. In contrast to microbes and animals, plants are able to synthesize all proteinaceous amino acids. As a result, the supplied labeled amino acid is diluted by endogenously synthesized amino acid and may also be catabolized and converted to other amino acids that are incorporated into protein. Differential uptake and internal fluxes of amino acids can lead to complex temporal labeling kinetics and inhomogenous labeling of proteins, depending on which amino acid is supplied (He et al., 1991). In a comparison of [^{2}H]Leu, [^{13}C]Arg, and [^{2}H]Lys labeling, Gruhler et al. (2005) concluded that all three substrates showed label dilution, and to varying extents. While stable isotopes of Lys are incorporated into the proteome with an enrichment of 83% to 91% in the dark, this falls to 58% in the light (Schütz et al., 2011). Another problem in plants is that labeled amino acids need to be added at high levels to generate a large increase in isotope abundance, which can alter metabolite pools and fluxes. Problems can also arise due to complex patterns of feedback regulation in amino acid biosynthesis pathways (Galili, 2002). In mammals, individual amino acids like Leu regulate and modify the rate of protein turnover (Buse and Reid, 1975; Pannemans et al., 1997). An additional complication in plants is that some amino acids are involved in further metabolic pathways. Examples include the use of Gly and Ser in photorespiration, Trp for auxin synthesis (Rapparini et al., 1999), and the aromatic amino acids Phe, Tyr, and Trp as precursors for the synthesis of phenylpropanoids and flavonoids (Fraser and Chapple, 2011).

Protein synthesis can also be measured using stable isotopes of water. Movement of label from $H_2{}^{18}O$ into amino acids is rather slow (Zhou et al., 2012). Label moves rapidly from ^2H_2O into amino acids and proteins (Mitra et al., 1976; Yang et al., 2010), but discrimination against ^2H_2O can lead to changes in metabolite pools and fluxes, to changes in gene expression indicative of stress, and to inhibition of growth (Thomson et al., 1963; Sacchi and Cocucci, 1992; Kushner et al., 1999; Yang et al., 2010). Yang et al. (2010) showed that inhibitory effects on growth can be decreased, although not totally prevented, by decreasing enrichment to 30% and that the stress-related changes in transcript levels were less marked when a protocol was used in which seedlings were pulsed with ^2H_2O and the labeling kinetics were analyzed in a chase with water. However, while ^2H_2O can be readily supplied to seedlings, movement through a larger plant is likely to be slow and rather heterogenous.

Another approach is to supply $^{15}NO_3$ or $^{15}NH_4$ to the medium of algae (Martin et al., 2012; Mastrobuoni et al., 2012) or the rooting medium of higher plants (Masclaux-Daubresse and Chardon, 2011; Nelson et al., 2014a, 2014b). Labeling with ^{15}N is especially useful in studies that use liquid chromatography-tandem mass spectrometry to analyze the labeling kinetics of signature peptides of individual proteins (Li et al., 2012; Nelson et al., 2014a, 2014b). However, there are some disadvantages in higher plants, including the rather slow labeling kinetics of amino acids (Yang et al., 2010). This may be due to the time that elapses until the label is transported through the plant and assimilated as well as to dilution by large internal pools (Lattanzi et al., 2005; Lehmeier et al., 2013). This also makes it difficult to rapidly and completely remove $^{15}NO_3$ or $^{15}NH_4$ in a chase.

Label can also be introduced as $^{13}CO_2$ in the atmosphere. This has three potential advantages. First, $^{13}CO_2$ is immediately incorporated into metabolism via photosynthesis, allowing the introduction of isotope into intact plants without any perturbation of metabolism and growth. Second, $^{13}CO_2$ and unlabeled CO_2 and be rapidly interchanged, allowing rapid commencement of

a pulse and rapid and complete removal of external label at the start of a chase. Third, at least in principle, $^{13}CO_2$ should label all amino acids. $^{13}CO_2$ labeling has been used to investigate fluxes in photosynthetic metabolism in algae (Huege et al., 2007; Young et al., 2011) and higher plants (Szecowka et al., 2013; Ma et al., 2014). It has also been used to investigate the synthesis and degradation of a small set of abundant proteins (Chen et al., 2011). However, quantitative measurements are complicated by slow and incomplete changes in enrichment in amino acids. In a recent study, we showed that the rate and extent of labeling of amino acids by $^{13}CO_2$ is highly variable; after a 60-min pulse, some amino acids like Ala were quite highly (more than 70%) labeled, others like Phe, Gly, and Ser were only moderately (20%–40%) labeled, and many, including Glu, Thr, Lys, Leu, Ile, Pro, and Asn, were very slowly and incompletely (less than 10%) labeled (Szecowka et al., 2013).

Here, we present a relatively simple approach that uses $^{13}CO_2$ pulse-chase analysis to measure the global rate of protein synthesis and degradation in intact soil-grown Arabidopsis plants. After labeling, gas chromatography time-of-flight mass spectrometry (GC-TOF-MS) is used to analyze enrichment in a large number of free amino acids and in their residues in protein. We identify which free amino acids show the cleanest labeling kinetics and use enrichment in these pools and the corresponding amino acid residues in protein to estimate the rates of protein synthesis and degradation. We also present a related method to quantify flux to cell wall polysaccharides.

RESULTS

Experimental Design

Szecowka et al. (2013) applied a pulse of $^{13}CO_2$ for various times up to 60 min, starting in the middle of the photoperiod after metabolic steady state had been achieved, to allow the computationally demanding modeling of fluxes in central metabolism. Based on the slow and incomplete labeling kinetics of amino acids by Szecowka et al. (2013) and estimates of the rate of protein synthesis based on ribosome abundance and usage (Piques et al., 2009), we reasoned that a longer pulse would be required to measure flux into protein. We decided to pulse for an entire day/night cycle and to chase for 4 d, taking samples at various times during this treatment. We also decided to commence labeling at dawn to minimize isotope dilution by internal pools, which are usually small at dawn (Gibon et al., 2006, 2009; Sulpice et al., 2014). In particular, starch is very low at dawn, accumulates in the light, and is remobilized to provide C for respiration and growth at night (Smith and Stitt, 2007; Stitt and Zeeman, 2012). By labeling from dawn onward, we hoped to achieve a high enrichment in starch that would allow high enrichment to be maintained in metabolites at night. To prevent dilution by dark fixation during the night, the $^{13}CO_2$ pulse was continued through until dawn.

Arabidopsis Columbia-0 (Col-0) plants were grown in a controlled climate chamber on soil under a short photoperiod (8 h of light/16 h of dark) for 18 d and transferred into two labeling chambers for 3 d before starting the labeling experiment. The labeling chambers were located inside the climate chamber, and each was large enough to hold 17 10-cm-diameter pots with five plants per pot. The chambers were flushed (5 L min^{-1}) with humidified air mixtures (79% N_2, 21% oxygen) containing 450 μL L^{-1} unlabeled or labeled CO_2. The CO_2 concentration reflected that measured in the climate chamber. The pulse was started by switching from unlabeled CO_2 to $^{13}CO_2$ just before dawn on day 21, and the chase was started by switching from $^{13}CO_2$ to unlabeled CO_2 at the following dawn. To prevent incorporation of label by plants that were being grown for subsequent experiments, the air mix exiting the labeling chamber was passed through a soda lime column. In routine experiments, plants were harvested at seven time points: at dawn just before starting the pulse (to measure natural enrichment), after 4 and 8 h in light, just before dawn at the end of the pulse, during the chase 4 h into first light period, and at dawn 1 and 4 d later. The extracts were separated into soluble and insoluble fractions and analyzed by GC-TOF-MS to determine enrichment in the individual free amino acids in the soluble fraction and, after chemical hydrolysis of the insoluble fraction, in the individual amino acids in protein. Although the analysis required only small amounts (20 mg fresh weight) of leaf material, for routine work, we typically pooled five rosettes per sample. In parallel, we measured the rate of rosette growth by weighing rosettes harvested at each sampled time point and by acquiring sequential images of the rosette area.

Enrichment Kinetics of Free Amino Acids

We were able to quantify enrichment in 16 free amino acids (Fig. 1; Supplemental Table S1A). The temporal kinetics of enrichment varies between amino acids and was often slow and incomplete. During the pulse, enrichment of individual amino acids ranged between 83% and 11% at the end of day and between 71% and 15% at the end of night. During the chase, enrichment decreased rapidly for some amino acids and slowly for others. This underlines the importance of information about enrichment in free amino acid pools for accurate estimation of the rate of protein synthesis.

We were searching for amino acids that showed a rapid increase to high enrichment in the light, retained high enrichment during the pulse in the night, and underwent a rapid and nearly complete decrease in enrichment in the chase. Ala showed the fastest and most complete increase of enrichment in the pulse (79%, 81%, and 65% after 4 and 8 h of illumination and at the end of night, respectively) and a rapid decrease in enrichment in the chase. Asp showed slightly lower enrichment. Ala and Asp are synthesized via reversible aminotransferase reactions from the central metabolites pyruvate and

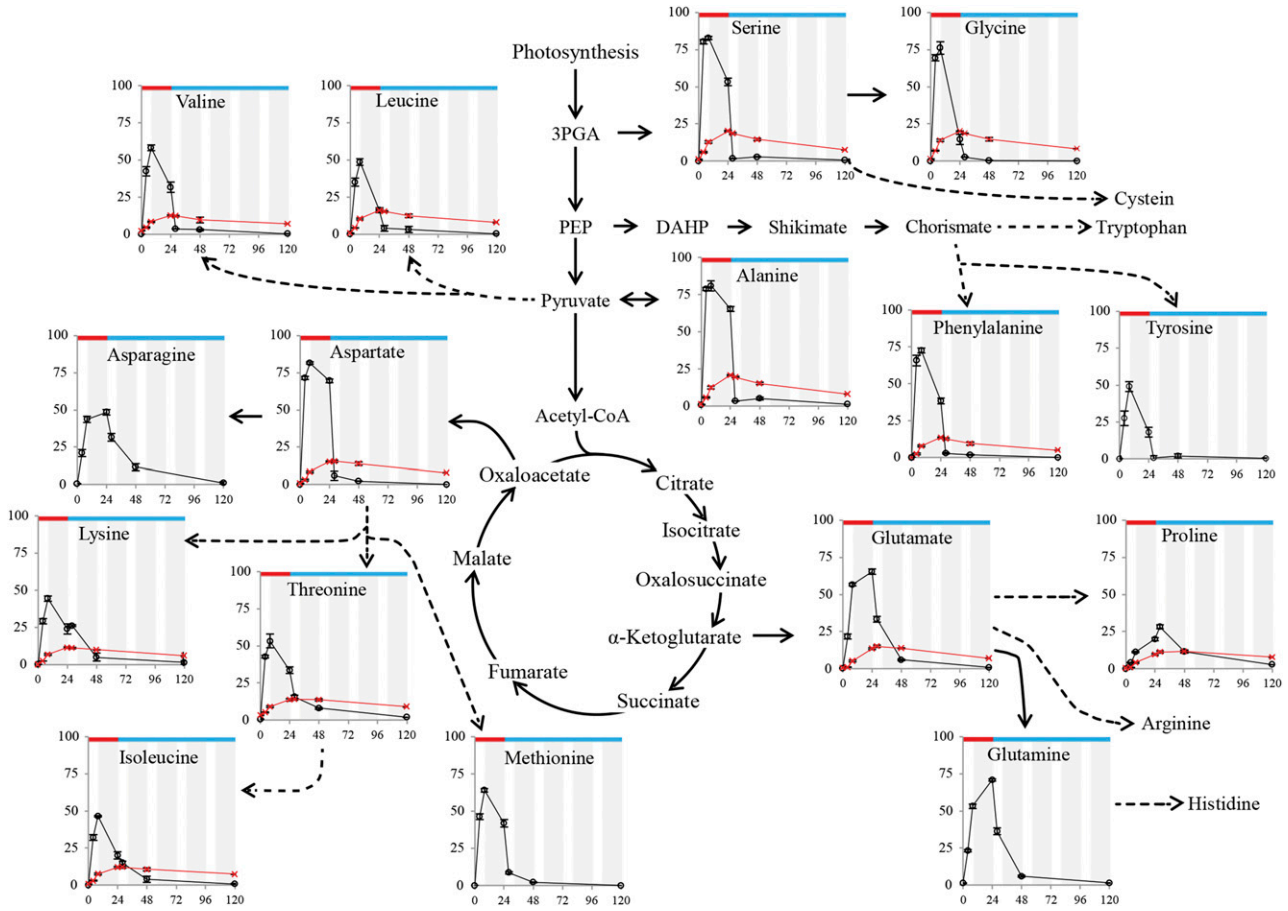

Figure 1. Enrichment kinetics of free amino acids and amino acids in protein in Col-0 growing in an 8-h photoperiod. The temporal kinetics of enrichment in 16 free amino acids (black lines) are shown as well as, for 12 of these, the kinetics of enrichment of the amino acid residue in protein (red lines).The *x* axis depicts time during the pulse and the chase (depicted with red and blue bars at the top of each graph, respectively). The *y* axis shows the percentage enrichment in the free amino acid or the amino acid residue in protein. The light period and night are indicated by white and gray shading, respectively. Col-0 was grown for 21 d in an 8-h photoperiod and then pulsed with $^{13}CO_2$ for 24 h, followed by a 4-d chase. Plants were harvested at dawn before the start of the pulse, after 4 and 8 h in the light, at the next dawn at the end of the pulse, at 4 h in the first light period of the chase, and at dawn at the end of days 1 and 4 of the chase. Each harvest comprised four pots, each containing five plants. The experiment was performed four times with separately grown batches of plants. The data are provided in Supplemental Data Set S1, the calculated enrichment in free amino acids and amino acids in protein in Supplemental Table S1, plots of individual isotopomers in Figure 2 and Supplemental Figure S2, and the calculated rates of protein synthesis and degradation in Table I. The plots show average (μ) of four biological replicates with SD ($\mu \pm$ SD). Error bars are omitted when they are smaller than the symbol. DAHP, 3-Deoxy-D-arabino-heptulosonic acid 7-phosphate; PEP, phospho*enol*pyruvate; 3PGA, 3-phosphoglyceraldehyde.

oxaloacetate, respectively. Ser and Gly also showed a rapid increase in enrichment in the light, but their enrichment decreased during the night (from 83% and 76% at dusk to 53% and 15% at dawn). Their rapid labeling in the light reflects their formation during photorespiration; reasons for the decline during the night will be discussed later. Glu and Gln showed relatively slow labeling in the light (22% and 22% after 4 h of illumination and 57% and 53% after 8 h of illumination, respectively) and a further rise during the night (65% and 71% at dawn, respectively). The slow labeling in the light was unexpected, because these amino acids are derived via aminotransferase reactions from the central organic acid α-oxoglutarate and are also intermediates in the GOGAT pathway, which is very active in the light (see "Discussion"). Most other amino acids are synthesized via long biosynthetic pathways. Enrichment in the aromatic amino acids (Phe and Tyr) rose quite quickly in the light and decreased rapidly in the chase, but they were labeled more slowly than Ala and also showed a marked decrease at night during the pulse. Ile, Leu, Lys, Met, and Val showed a gradual increase in enrichment during the light period, incomplete enrichment at dusk (44%–58%), a decrease in enrichment at night during the pulse, and a slow decrease in enrichment during the chase. The slowest labeling kinetic was found for Pro.

Slow and incomplete labeling kinetics can result for several reasons, including dilution of label by internal pools, synthesis of amino acids from unlabeled precursors, or the presence of compartmented pools with different labeling kinetics. We inspected our data to provide insights into the contribution of these different factors.

Our GC-TOF-MS analysis provided information about enrichment in sugars and organic acids (Supplemental Fig. S1; Supplemental Table S1A). Labeling of malate was rapid and high in the pulse (73%, 79%, and 79% after 4 and 8 h of illumination and at the following dawn, respectively) and decreased rapidly in the chase. Enrichment was slightly lower in fumarate and succinate. Enrichment of pyruvate was high in the light (71% and 77% after 4 and 8 h, respectively), declined at night (35%), and declined rapidly in the chase. Enrichment in citrate was very low in the light (less than 1%), rose strongly in the night (52%), remained at this level for the first 4 h of the chase in the light, and decreased by the following dawn. The slow labeling of Glu and Gln in the light may be a consequence of the slow labeling of citrate (see "Discussion"). Labeling of Suc and reducing sugars was slow and incomplete in the pulse and declined slowly in the chase. They may provide a source of unlabeled C in the night.

We inspected the detailed labeling pattern of each amino acid to learn whether there are strongly compartmented pools of any of the amino acids. If an amino acid occurs as a single pool or as multiple pools that are in relatively rapid exchange, during the pulse the unlabeled C0 isotopomer (i.e. all C atoms are unlabeled) will decrease to a low value, intermediate isotopomers with a low number of ^{13}C atoms will rise transiently and then decrease to a low value, and heavily labeled isotopomers that consist predominantly or entirely of labeled atoms will rise to a high value. This pattern is seen in the light for Ala (Fig. 2A), Gly, Ser, and Asp (Supplemental Fig. S2) and, somewhat more slowly, for Met. If incomplete labeling of an amino acid is due to slow labeling of one pool, the same pattern will be followed, but more slowly. This pattern is seen for Glu (Fig. 2B) and Gln (Supplemental Fig. S2). If incomplete labeling is due to the presence of two or more pools, of which one or more is not labeled or is only very slowly labeled, the C0 isotopomer will decrease to an intermediate value, and the remainder of the pool will be present as heavily labeled isotopomers. This pattern was seen at dusk for Lys (Fig. 2C), Pro, Tyr, Phe, Val, Leu, and Ile (Supplemental Fig. S2).

We also investigated whether some amino acids were present at a much higher level at dusk than at dawn. Such diurnal changes are due probably to synthesis of the amino acid from newly fixed C in the light and use of this pool at night. This will lead to any compartmented unlabeled pools making only a small contribution to the total pool at dusk but a large contribution at dawn. This analysis was only possible for the amino acids for which standards were included in the GC-TOF-MS analysis to allow quantification. There

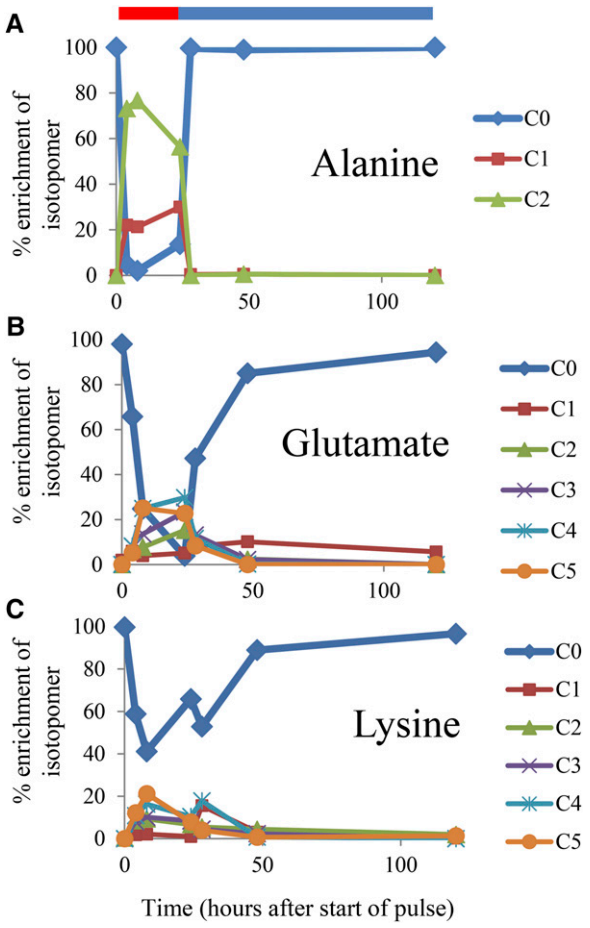

Figure 2. Labeling kinetics for all detected isotopomers of the free amino acid pools. A, Ala. B, Glu. C, Lys. C0, C1, C2, C3, and CX correspond to the isotopomer with no ^{13}C atoms (i.e. all atoms are unlabeled), with one ^{13}C atom, with two ^{13}C atoms, with three ^{13}C atoms, and with x ^{13}C atoms, respectively. The experimental design is described in the legend of Figure 1. The data are provided in Supplemental Data Set S1, and the calculated enrichment values are provided in Supplemental Table S1.

was an especially large increase for the photorespiratory intermediate Gly (37-fold) and a smaller increase for Ser (3.7-fold; Supplemental Table S2). Based on other studies, we can also expect a large diurnal change for Gln (Foyer et al., 2003; Fritz et al., 2006; Tschoep et al., 2009).

Enrichment Kinetics of Amino Acids in Protein

GC-TOF-MS analysis of the protein hydrolysate provided enrichment data for 12 amino acids (Fig. 1; Supplemental Table S1B; Gln, Asn, Met, and Tyr could not be reliably detected in the hydolysate). In total, 12 amino acids were detected in both the free and protein pools.

Enrichment of amino acids in protein increased during the pulse in the light and rose further in the night,

Table I. *Estimated rates of protein synthesis and degradation for Col-0 grown in an 8-h photoperiod*

Col-0 was grown for 21 d in an 8-h photoperiod and then pulsed with $^{13}CO_2$ for 24 h, followed by a 4-d chase. The experimental design is described in the legend of Figure 1. The data are provided in Supplemental Data Set S1 and calculated enrichment values in Supplemental Table S1. The rate of protein synthesis was calculated by correcting enrichment in Ala in protein by the enrichment in free Ala at the end of the day. The calculations of protein degradation used an RGR of 0.221 mg fresh weight mg^{-1} fresh weight d^{-1}, which was the average of three biological replicate experiments in these growth conditions (Supplemental Fig. S5). Results are estimated from the average of four biological replicates.

RGR	Protein Synthesis				Protein Degradation		Half-Life	
	Average 24-h Cycle	Light (per Hour)	Dark (per Hour)	Light:Dark Ratio	Pulse	Chase	Pulse	Chase
mg mg^{-1} d^{-1}	*% total protein*				*% total protein d^{-1}*		*d*	
0.221	25.62	1.95	0.63	3.1	3.52	3.07	3.11	3.49

although more slowly than in the light. This provides qualitative evidence that protein synthesis continues at night. Enrichment at the end of the 24-h pulse varied more than 2-fold, depending on the amino acid. Like free amino acids, the highest enrichment was found for Ala, Gly, and Ser (20.7%, 20.1%, and 20.2%, respectively), with somewhat lower enrichment in Asp (15.4%). The lowest enrichment was for Pro (8.3%).

We investigated whether these differences in enrichment in protein could be explained by the differences in average enrichment of the free amino acids. To do this, we plotted the increase in enrichment of the amino acid in protein during the light period against the enrichment in the free amino acid pool at dusk (Supplemental Fig. S3A). A similar plot was made comparing the increase in enrichment of the amino acid in protein during the night with the enrichment in the free amino acid pool at dawn (Supplemental Fig. S3B). A small group of amino acids showed high enrichment in the free pool and a high rate of incorporation into protein. This group included Ala in the light and dark, Ser in the light and dark, Gly in the light, and Glu in the dark. Another group, including Asp in the light and dark and Phe and Glu in the light, showed slower label incorporation into protein than expected from the enrichment in the free pool. This may reflect slow labeling kinetics, which would result in the average enrichment of the free pool at dawn or dusk being higher than the average during the preceding time interval. Another group, including Lys and Pro in the light and Gly, Pro, Leu, Ile, and Lys in the dark, showed higher label incorporation into protein than expected from enrichment in the free amino acid. This might be explained by the presence of a weakly labeled or unlabeled pool, with the result that the actual precursor pool has a higher enrichment than the average value. Another group, including Thr and Val in the light and dark, Leu and Lys in the light, and Phe in the dark, showed a similar relationship to Ala and Ser, but with lower enrichment and lower incorporation rates into protein. While this might indicate that there is one slowly labeled pool of these amino acids, inspection of the labeling kinetics of their isotopomers (see above; Supplemental Fig. S2) makes it more likely that the situation is actually more complex, with a combination of slow labeling kinetics for one pool and the presence of a weakly or unlabeled pool. Overall, this analysis and that of Figures 1 and 2 and Supplemental Figures S2 and S3 suggest that multiple factors contribute to the complex labeling kinetics of free amino acids.

The washout kinetics in protein during the chase were analyzed with semilog plots (Supplemental Fig. S4). Ala, Ser, and Gly had the fastest washout (slopes of −0.23, −0.24, and −0.21), with smaller slopes for other amino acids (−0.18 to −0.11 and even slower for Pro). This shows that, for many amino acids, incomplete loss of label in free pools complicates protein labeling kinetics during the chase.

Determination of the Relative Growth Rate

Estimation of the rate of protein degradation requires information about the rate of growth. Growth rates are usually given as the relative growth rate (RGR), which is the gain in biomass per unit of existing biomass per day (Poorter and Nagel, 2000). We measured RGR by fitting a regression to a semilog plot of the fresh weight of the plants harvested during the pulse and chase. Such measurements are subject to experimental error because different plants are harvested at each time point and weight varies between individual plants. This could affect the accuracy of our calculation of protein degradation. We took two approaches to validate our estimates of RGR. First, we took sequential images of sets of plants grown in parallel with those that were used for destructive analyses. Destructive harvesting and time-lapse image analysis were in good agreement; in this experiment, they provided estimates for RGR of 0.224 and 0.215 $mm^2\ mm^{-2}\ d^{-1}$, respectively (Supplemental Fig. S5). Second, we determined RGR by destructive harvesting in three separate large experiments performed on plants growing in the same conditions during the time when we were carrying out our labeling studies. The values were very similar (average $[\mu] \pm SD = 0.221 \pm 0.002$; Supplemental Fig. S5). For routine estimates of protein degradation, we used the average estimate of RGR from all these replicated experiments.

Estimation of the Rate of Protein Synthesis and Degradation

The rate of protein synthesis, K_s, was estimated from label incorporation into Ala in protein, with a correction

for enrichment in free Ala (see "Discussion"; Pocrnjic et al., 1983) using the equation:

$$Ks = \frac{\langle S_B(t_2)\rangle - \langle S_B(t_1)\rangle}{\langle S_{A(t_2 - t_1)}\rangle} \times \frac{100}{t_2 - t_1} (\%\ \text{per h})$$

where $\langle S_B(t_1)\rangle$ and $\langle S_B(t_2)\rangle$ represent average label incorporation into Ala in protein at the start and end of the analyzed time interval, $\langle S_{A(t_2 - t_1)}\rangle$ is the average enrichment of free Ala at the end of the light period (see "Discussion"), and $(t_2 - t_1)$ is the duration of the time interval in hours. The rate of synthesis is given as the percentage of the initial protein synthesized in the time interval. To calculate the rate of protein synthesis rate in the light period, t_2 was the end of the light period (8 h), and t_1 was the start of the pulse (0 h). To calculate protein synthesis rate in the dark, t_2 was the end of the 24-h pulse, and t_1 was the end of the light period (8 h).

The estimated rate of protein synthesis in the light period (1.95% h^{-1}) was about 3-fold higher than that at night (0.63% h^{-1}). However, as the plants were in an 8-h photoperiod, the amount of protein synthesized at night was 61% of that synthesized in the light period. The protein synthesized during a 24-h cycle was equivalent to about 26% of the protein in the rosette.

The rate of protein degradation, K_d, was estimated in two ways. The first approach is based on the difference between the estimated rate of protein synthesis in the pulse, K_s, and the rate of protein synthesis needed to sustain the observed rate of growth. It is calculated as:

$$Kd = (Ks - \text{RGR} \times Pp) \times 100\ (\%\ \text{per d})$$

where P_p is the fractional change in rosette protein content per day during the pulse. The second approach calculates the rate of protein degradation as the difference between the measured decrease in enrichment in Ala in protein during the chase and the decrease that would be expected due to dilution by growth (Yee et al., 2010) as:

$$Kd = (-k_{Loss} - \text{RGR} \times Pc) \times 100\ (\%\ \text{per d})$$

where k_{Loss} is the rate constant for the loss of label in Ala in protein per day and P_c is the fractional change in rosette protein content per day during the chase. k_{Loss} was calculated for Ala by applying linear regression of the natural log-transformed enrichment value versus time over at least three time points. The very low enrichment in free Ala during the chase allowed us to ignore recycling of label into protein. The rosette protein concentration did not change significantly between days 19 and 26 after germination (Supplemental Data Set S1). This allowed us to set the protein concentration terms (P_p and P_c) at unity for the calculation of protein degradation in rosettes.

The rate of protein degradation (i.e. protein synthesis in excess of that required for growth) per 24-h cycle was estimated at 3.5% d^{-1} from the pulse data and 3.1% d^{-1} from the chase data. Thus, the majority of the protein synthesis (26% d^{-1}) represents flux to growth, rather than degradation. Combining the dilution of protein by growth with the rate of protein degradation yielded a global protein half-life of 3.1 to 3.5 d.

Different Leaf Growth Stages

We next applied this method to investigate the rate of protein synthesis and degradation at different stages of leaf development. Ribosome abundance (Dean and Leech, 1982) and, by implication, the rate of protein synthesis are high in young growing leaves and low in mature leaves. Leaves at six stages of development (Fig. 3A) were harvested at the beginning and end of a 24-h pulse and processed to provide information about the enrichment of free amino acids and of amino acids in protein (Supplemental Data Set S2). As large numbers of plants were required to provide enough material for the young leaves, we did not attempt to separate fluxes in the light period and night. We did not apply a chase over 4 d because in this time the leaves will change their developmental stage. Leaf relative growth rate (LRGR) was estimated from images of individual leaves on sequential days spanning the pulse (Fig. 3B). It should be noted that the oldest leaves are still growing slowly. The rate of protein synthesis was calculated from the average enrichment of free Ala (81%) in a subsample of whole rosettes harvested at the end of the light period. This was validated by checking that Ala enrichment at dawn at the end of the pulse was similar in all six leaf stages at dawn at the end of the pulse (Fig. 3C) but lower than at dusk, as was seen previously. The estimated rate of protein synthesis was fastest (42.8% d^{-1}) in the youngest rapidly growing leaf (LRGR = 0.48) and lowest (15.6%–16% d^{-1}) in the oldest leaves (LRGR = 0.12–0.13; Fig. 3D; Supplemental Table S3).

To calculate protein degradation, we compared the rate of protein synthesis with the amount of protein required for growth. In this case, it was necessary to include information about the decrease in protein concentration during leaf development. The daily decrease in protein concentration at each leaf stage was estimated in a separate experiment, in which the rate of leaf initiation was scored and leaves 1 to 6 were harvested from 21-d-old plants to determine fresh weight and protein concentration at each leaf stage (Supplemental Data Set S2). The decrease in leaf protein was estimated as 12%, 15%, 1%, and 16% d^{-1} for leaves 6, 5, 4, and 3, respectively. The estimated requirement for protein for growth decreased from about 42% d^{-1} in the youngest leaves to 12% d^{-1} in the oldest leaves (Fig. 3D). At all leaf stages, most of the protein synthesis represented flux to growth (Fig. 3D). The estimated rate of protein degradation was negligible in the young leaves and about 8%, 3%, and 4% d^{-1} in leaves 3, 2, and 1, respectively. The estimates

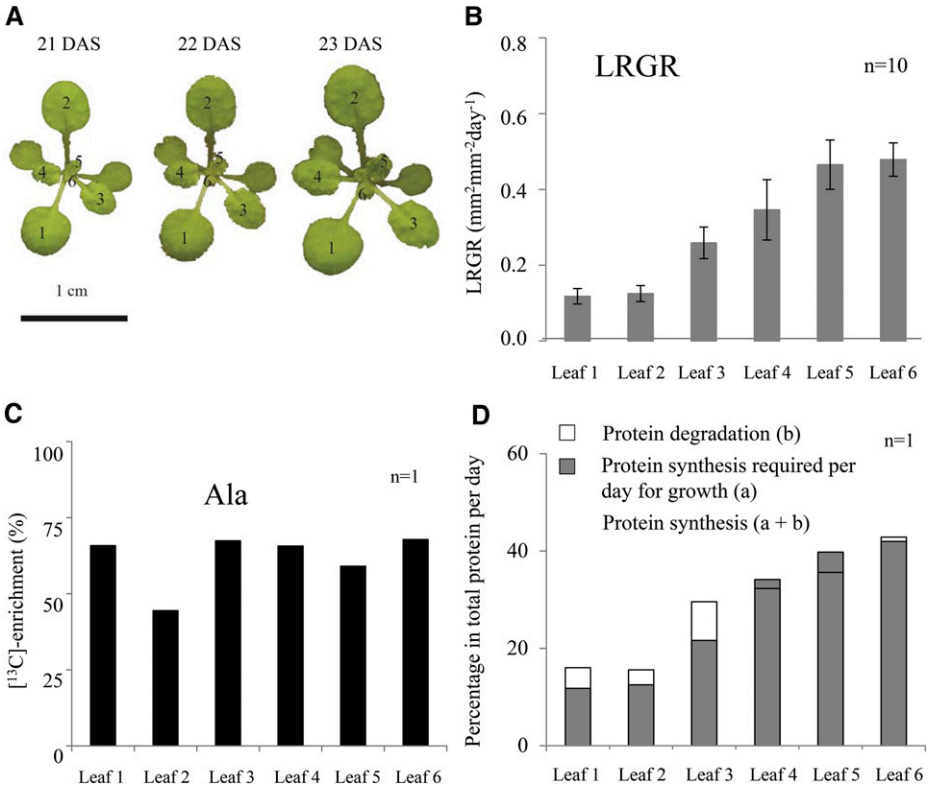

Figure 3. Leaf growth rates, protein synthesis rates, and protein degradation at different stages of leaf development. Col-0 was grown for 21 d in an 8-h photoperiod and then pulsed with $^{13}CO_2$ for 24 h. Plants were harvested at dawn before the start of the pulse and at dawn at the end of the pulse and separated into leaf stages for further analysis. Each sample consisted of 20 leaves from 20 plants. A, Images of a typical plant at 21, 22, and 23 d after sowing (DAS). The numbers on the leaves correspond to leaf numbers on the *x* axes in B to D. B, LRGR at each leaf stage during the chase, estimated from sequential images of the rosette from three plants. C, Enrichment values of free Ala for each leaf stage at the end of the pulse from a sample of 20 pooled leaves. D, Comparison of the estimated rate of protein synthesis and the rate of protein synthesis that was required for growth. The complete bar (a + b) represents the rate of protein synthesis, estimated from enrichment in Ala in protein corrected for enrichment with free Ala. The gray bar (a) represents the rate of protein synthesis required for growth. This was calculated from LRGR corrected for the decrease in protein per day in a leaf at that stage. The rate of protein degradation (b) was calculated as the difference between the rate of protein synthesis and the amount of protein required for growth. The data, including estimated changes in leaf protein content with time, are provided in Supplemental Data Set S2. Calculated values for protein synthesis and degradation are provided in Supplemental Table S3.

in young leaves are subject to error because they represent the difference between two large values, both of which are susceptible to experimental noise. The values found in the mature leaves resemble those seen in a mature rosette, as expected because mature leaves contribute most of the rosette biomass.

Higher Growth Temperature

High temperature results in an increase in respiration, especially maintenance respiration (Penning de Vries et al., 1979; Amthor, 2000; Pyl et al., 2012). While the main maintenance costs are thought to include protein turnover and the maintenance of electrical, pH, and ion gradients across membranes (Penning de Vries, 1975; Amthor, 2000), they are difficult to quantify from molecular information (Amthor, 2000; Cheung et al., 2013; Sweetlove et al., 2014). We applied our method to investigate whether higher temperature leads to a major increase in the rate of protein degradation.

We grew Arabidopsis in an 8-h photoperiod at 20°C or 28°C for 21 d, applied a $^{13}CO_2$ pulse for 24 h, harvested plants at dawn at the end of the pulse and after a 1-, 2-, 3-, or 4-d chase, determined the enrichment of free Ala and of Ala in protein, and estimated the rate of protein synthesis and, by comparison with parallel measurements of RGR, the rate of protein degradation (Table II; data provided in Supplemental Data Set S3). Protein synthesis was 15% higher at 28°C than at 20°C (Table II). As we did not collect samples at dusk, we used the enrichment data at dawn to estimate protein synthesis rates. This may result in a slight overestimation, because enrichment in free Ala decreases slightly during the night. For this reason, we did not attempt to use data from the pulse to estimate degradation rates.

Table II. *Protein degradation in Arabidopsis grown at 20°C and 28°C*

Col-0 was grown for 21 d in an 8-h photoperiod at either 20°C or 28°C, then pulsed with $^{13}CO_2$ for 24 h, followed by a 4-d chase. Plants were harvested at dawn before the start of the pulse, at dawn at the end of the pulse, and at dawn after 1, 2, 3, and 4 d of chase. The data are provided in Supplemental Data Set S3. Three or four samples of five plants were harvested at each time point for 28°C or 20°C, respectively. The rate of protein synthesis was estimated from the ^{13}C enrichment in protein in Ala at the end of a 24-h pulse and normalized with the enrichment in free Ala at the end of the pulse. The rate of protein degradation was estimated by comparing the decrease in enrichment in Ala in protein during the chase with RGR. This normalization will lead to a slight overestimation of the protein synthesis. The RGR at 20°C is the mean of three biological experiments, and that at 28°C is the mean of three biological replicates. Results are estimated from the average of four biological replicates from 20°C-grown plants and the average of three biological replicates from 28°C-grown plants.

Treatment	RGR	Protein Synthesis	Protein Degradation	Half-Life
	mg mg^{-1} d^{-1}	*% d^{-1}*		*d*
20°C	0.221	31.7	3.07	3.49
28°C	0.244	37.3	3.70	2.99
Ratio 20°C:28°C	0.91	0.85	0.83	

Degradation rate estimated from the chase showed a 17% increase at 28°C compared with 20°C (3.7% and 3.1% d^{-1}, respectively). Thus, protein synthesis and protein degradation increase by approximately the same extent between 20°C and 28°C.

Nucleus-Encoded Large Subunit and Plastid-Encoded Small Subunit of Rubisco

We were interested to learn if our approach could be adapted to measure the synthesis and degradation of individual proteins. For this, we focused on the highly abundant protein Rubisco (Eckardt et al., 1997). Rubisco consists of a nucleus-encoded small subunit (RBCS) and a plastid-encoded large subunit (RBCL). Almost half of the ribosomes in leaves are located in the plastid (Detchon and Possingham, 1972; Dean and Leech, 1982; Piques et al., 2009). They are involved in the synthesis of plastid-encoded proteins, including RBCL and components of complexes in the thylakoid membrane. It is generally thought that plastid protein synthesis is inhibited in the dark (Marín-Navarro et al., 2007). In agreement, at night there is a larger decrease in loading of plastid ribosomes than cytosolic ribosomes into polysomes (Piques et al., 2009; Pal et al., 2013).

Arabidopsis Col-0 was pulsed with $^{13}CO_2$ for 24 h, harvested at dusk and dawn, and applied to SDS-PAGE, and the 52- and 18-kD bands were eluted and chemically digested (Allen et al., 2012) for analysis with GC-TOF-MS (Supplemental Data Set S4). Synthesis rates were calculated using enrichment in free Ala, assuming that there is similar enrichment in the cytosol and plastid. In the light, synthesis was faster for RBCL (1.2% h^{-1}) than for RBCS (0.80% h^{-1}), although the difference was not statistically significant (P = 0.13). Synthesis rates were lower at night but similar for RBCL and RBCS (0.37 and 0.36% h^{-1}, respectively; Table III). The decrease in RBCL synthesis between light and dark (3.2-fold) resembled the decrease in the global rate of protein synthesis (Table I). Thus, RBCL translation is not preferentially inhibited in the dark.

The Starchless *phosphoglucomutase* Mutant

In a last application, we investigated protein synthesis and degradation in the starchless *phosphoglucomutase* (*pgm*) mutant. Analysis of transcript and metabolite profiles has revealed that *pgm* starves at night in short photoperiods (Gibon et al., 2004b, 2006; Usadel et al., 2008). We posed two questions. First, how strongly is protein synthesis inhibited in *pgm* at night? Analysis of polysome loading using density gradient centrifugation (Pal et al., 2013) showed that some polysomes are still present at night in *pgm*, although fewer than in Col-0. We wanted to distinguish between two explanations for this observation: that despite extreme C starvation, there is still a low rate of protein synthesis or that the ribosomal RNA retrieved in the polysome fraction in *pgm* at night is not in active polysomes. Second, based on an increase in the levels of minor amino acids in the night in *pgm*, it has been proposed that protein catabolism is activated (Gibon et al., 2004b, 2006; Izumi et al., 2013). This should be detectable as a higher rate of protein degradation. We would also expect a faster decay of the enrichment in free amino acids in the night, due to increased recycling of predominantly unlabeled amino acids from protein.

The *pgm* mutant grows very poorly in short-day conditions. For this reason, we grew the mutant initially in a 12-h photoperiod before transferring it to an 8-h photoperiod, also increasing the duration of the growth period to obtain a rosette biomass similar to that in 21-d-old wild-type Col-0. Wild-type Col-0 and *pgm* were then exposed to a 24-h $^{13}CO_2$ pulse and a 4-d chase, harvesting at dawn before the start of the pulse, at dusk, 4 h into the night, at dawn, and after a 4-d chase (for original data, see Supplemental Data Set S5; for enrichment data, see Supplemental Table S4). The time point at 4 h into the night was included because

Table III. *Synthesis rate of RBCL and RBCS in the light period and the night*

Col-0 was grown for 21 d in an 8-h photoperiod and then pulsed with $^{13}CO_2$ for 24 h. Plants were harvested at dusk and at dawn at the end of the pulse. Protein was separated by PAGE, and bands corresponding to RBCL and RBCS were eluted and analyzed. The data are provided in Supplemental Data Set S4. The results are given as means ± SD (n = 3 biological replicates except for RBCS in the dark, where n = 2).

Protein Synthesis Rate	RBCL		RBCS		Light:Dark Ratio	
	Light	Dark	Light	Dark	RBCL	RBCS
Per period (%)	9.27 ± 1.01	5.84 ± 1.05	6.40 ± 3.21	5.75 ± 2.70	1.59	1.11
Per hour (%)	1.16 ± 0.13	0.37 ± 0.07	0.80 ± 0.40	0.36 ± 0.17	3.17	2.23

pgm accumulates high levels of sugars in the light and depletes them during the first 3 to 4 h of the night (Gibon et al., 2004b, 2006). C starvation is unlikely to develop until after this time; indeed, polysome loading decreases gradually in parallel with the depletion of sugars during the first hours of the night (Pal et al., 2013).

Enrichment in free amino acids increased in a similar manner in Col-0 and *pgm* in the light but decayed about 2-fold more rapidly in *pgm* from 4 h onward in the night, pointing to rapid protein degradation in the night (for Ala, see Fig. 4; for other amino acids, see Supplemental Fig. S6). The only exception was Asn, whose enrichment increased at night in *pgm* (see "Discussion").

The estimated rates of protein synthesis and degradation are summarized in Table IV. For Col-0, the absolute rates and the changes between the light period and the night resemble those in the experiment of Table I. For *pgm*, the rate of protein synthesis in the light was slightly but not significantly lower than that of Col-0 (1.8% and 2.1% h^{-1}, respectively). The rate of protein synthesis decreased in the first 4 h of the night but was similar to that in Col-0 (0.54% and 0.68% h^{-1}, respectively). In the remainder of the night, the rate decreased further in *pgm* (0.29% h^{-1}) but was maintained in Col-0 (0.7% h^{-1}). The rate of protein synthesis over the entire 24-h cycle was 29% lower in *pgm* (18% d^{-1}) than in Col-0 (25.3% d^{-1}). Comparison of the average protein synthesis rate with RGR revealed a higher average rate of protein degradation in *pgm* than in Col-0 (4.3% compared with 3.2% d^{-1}, respectively). Analysis of the chase yielded slightly higher degradation rates for both genotypes but confirmed that degradation was faster in *pgm* than in wild-type Col-0 (6.1% and 4.8% d^{-1}, respectively).

In summary, *pgm* has a 29% lower rate of protein synthesis per 24 h than Col-0, due to a lower rate of protein synthesis in the second part of the night. The rate of protein degradation over a 24-h cycle is higher, especially when related to the rate of protein synthesis; daily average protein degradation is equivalent to 24% to 34% of daily average protein synthesis in *pgm*, compared with 13% to 19% in Col-0. The lower rate of synthesis and higher rate of degradation result in an almost 2-fold decrease in the net gain of protein per day (11.9%–13.7% d^{-1} in *pgm* compared with 20.5%–22.1% d^{-1} in Col-0). These estimated net rates of protein synthesis are very similar to RGR estimated from changes in plant size (0.221 and 0.137 mg mg^{-1} d^{-1}, respectively, in Col-0 and *pgm*).

Estimation of Growth by Measuring Enrichment in Glc in the Cell Wall

In a last set of experiments, we investigated whether $^{13}CO_2$ labeling can be used to estimate the rate of cell wall synthesis. We did this for two reasons: first, to compare the rates of cell wall synthesis with those of protein synthesis; and second, as an alternative way of

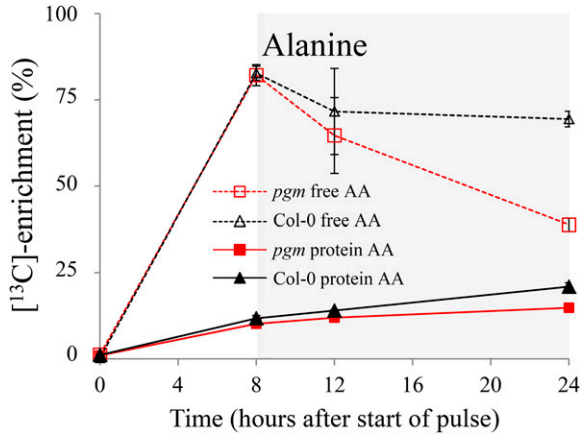

Figure 4. Enrichment in free Ala and in Ala residues in protein in wild-type Col-0 and the starchless *pgm* mutant. The *pgm* mutant was grown for 25 d in a 12-h photoperiod and shifted to an 8-h photoperiod 3 d prior to the experiment. Col-0 was grown for 21 d in an 8-h photoperiod. Col-0 and *pgm* were pulsed with $^{13}CO_2$ for 24 h, followed by a 4-d chase. Plants were harvested at five time points: at dawn before the start of the pulse, at dusk, 4 h into the night, at dawn at the end of the pulse, and at dawn after a 4-d chase (data not shown). The data are provided in Supplemental Data Set S5, enrichment in free amino acids and amino acids in protein in Supplemental Table S4, and estimated rates of protein synthesis and protein degradation in Table IV. The experiment was repeated three times, taking one sample of five plants at each time point in each experiment. The plot shows average (μ) of three biological replicates with SD (μ ± SD). The absence of error bars means that they were smaller than the symbols. The increase in enrichment in amino acids in protein in *pgm* between 4 and 16 h into the night was significant (P = 0.016). AA, Amino acid.

Table IV. *Comparison of the rates of protein synthesis and degradation in Col-0 and the starchless pgm mutant*

Col-0 was grown for 21 d in an 8-h photoperiod. *pgm* was sown out 7 d earlier than Col-0 and initially grown in a 12-h photoperiod to allow the acquisition of biomass, before transfer to an 8-h photoperiod 3 d before the start of the pulse. Both genotypes were pulsed with $^{13}CO_2$ for 24 h, followed by a 4-d chase. Plants were harvested at dawn before the start of the pulse, at dusk, 4 h into the night, at dawn at the end of the pulse, and at dawn after a 4-d chase. The experiment was repeated three times with separately grown batches of plants; in each experiment, one sample of five plants was harvested at each time point. Rates of synthesis were estimated for two time intervals in the night: between dusk and 4 h of darkness (T8–T12) and between 4 h of darkness and the end of the night (T12–T24). The data are provided in Supplemental Data Set S5, calculated enrichments in Supplemental Table S4, and plots of changes in the enrichment of selected amino acids in Figure 4. The rate of protein synthesis was calculated by correcting enrichment in Ala in protein by the enrichment in free Ala at dusk. Results are estimated from the average of three biological replicates.

Plant	RGR	Protein Synthesis				Protein Degradation		Half-Life	
		Average per 24-h Cycle	Light (T0–T8) per Hour	Dark (T8–T12) per Hour	Dark (T12–T24) per Hour	Pulse	Chase	Pulse	Chase
	mg mg^{-1} d^{-1}	*% total protein d^{-1}*						*d*	
Col-0	0.221	25.29	2.11	0.68	0.7	3.18	4.84	3.38	2.48
pgm	0.137	18.02	1.81	0.54	0.29	4.33	6.09	2.67	2.17
Ratio *pgm*:Col-0	0.62	0.71	0.86	0.8	0.42	1.36	1.26		

estimating RGR. Up to 55% of Arabidopsis rosette dry weight is cell wall (Williams et al., 2010), of which about 20% to 30% is cellulose, with further contributions from hemicellulose, pectin, and proteins (Somerville et al., 2004; Lodish et al., 2011; Somerville et al., 2004). Cellulose and the backbone of hemicellulose consist of β(1-4)-linked D-Glc. Assuming that there is little or no degradation of these polysaccharides, enrichment in Glc in the cell wall should be a reasonable proxy for the rate of growth.

Using material from the experiment of Table IV, cell walls were isolated, thoroughly digested to remove starch, chemically hydrolyzed, and analyzed by GC-TOF-MS to determine the kinetics of enrichment in Glc in the cell wall (Tables V and VI). In this case, we did not apply a correction for incomplete labeling of precursor. Hexose phosphates and UDP-Glc show quite complex labeling kinetics due to the presence of compartmented pools (Szecowka et al., 2013). Suc-6-P, which lies downstream of these metabolites, is rapidly labeled to more than 70% enrichment, giving a minimum value for enrichment in the hexose phosphate and UDP-Glc precursor pools (Szecowka et al., 2013).

In the light period, the rate of label incorporation into Glc in the cell wall is about 50% faster in Col-0 than in *pgm* (1.52% and 1.01% h^{-1}, respectively). During the first 4 h of darkness, growth decreased in Col-0 but remained high in *pgm* (0.45% and 1.3% h^{-1}, respectively). It should be noted that there were relatively small changes in enrichment in this short time interval, so the estimated rates are less reliable than for other time intervals. In the remainder of the night, Glc incorporation continued at the same rate in Col-0 but stopped in *pgm* (0.44% and 0.02% h^{-1}, respectively). In wild-type Col-0, the decrease in the rate of cell wall synthesis in the night compared with the light period (about 3-fold) is similar to the decrease in the rate of protein synthesis. In contrast, in *pgm*, cell wall synthesis is almost completely inhibited in the last part of the night, whereas (see above) protein synthesis continues at a low rate.

We used the labeling kinetics of Glc in the cell wall to estimate the relative rate of accumulation of structural dry matter (RGR^{STR}), assuming that there is no degradation of Glc in cell wall polysaccharides (Tables V and VI; Supplemental Data Set S5). Summing the rates of Glc incorporation estimated from the pulse data gave estimates of RGR^{STR} of 0.192 and 0.135 in Col-0 and *pgm*, respectively (Tables V and VI). The labeling kinetics in the chase allowed an independent estimate of RGR^{STR} as:

$$RGR^{STR} = \sqrt[t]{\frac{x}{y}} - 1$$

where x and y are enrichment in Glc in cell wall at the end of the pulse and the end of the chase, respectively, and t is the duration of the chase in days. This approach gave estimates of RGR^{STR} of 0.205 in Col-0 and 0.127 in *pgm* (Tables V and VI). Both approaches yield estimates of RGR^{STR} that are slightly lower than RGR obtained by an analysis of plant size (0.221 and 0.137 mg mg^{-1} d^{-1} in Col-0 and *pgm*, respectively). The slightly lower RGR^{STR} obtained by an analysis of enrichment in cell wall Glc compared with RGR estimated from changes in plant size might be due to enrichment in metabolites in central metabolism saturating at about 90% (Szecowka et al., 2013). Despite this slight discrepancy, RGR^{STR} and RGR showed similar decreases (both about 38%) in *pgm* compared with Col-0.

DISCUSSION

A Simple Protocol to Measure the Global Rate of Protein Synthesis and Degradation in Whole Plants Growing in a Light/Dark Cycle

We have established a simple method to quantify the global rate of protein synthesis and protein degradation. By providing $^{13}CO_2$ in the atmosphere in the

Table V. *Rate of cell wall synthesis in Col-0 and the starchless pgm mutant*

Changes in enrichment in Glc in the cell wall fraction in different time intervals during a day-night cycle and during the entire 24-h $^{13}CO_2$ pulse are shown. The data are for the same experiment as that of Table IV. The original data are provided in Supplemental Data Set S5.

Time	Increase in Enrichment per Interval		Increase in Enrichment per Hour		Ratio Col-0:*pgm*
	Col-0	*pgm*	Col-0	*pgm*	
	%				
T0 to T8 (light)	12.15	8.06	1.52	1.01	1.51
T8 to T12 (start of night)	1.79	5.12	0.45	1.28	0.35
T12 to T24 (later in night)	5.29	0.29	0.44	0.02	18.54
T0 to T24	19.23	13.47			

light, we rapidly introduce label in the pulse and remove it during a chase without perturbing metabolism and growth. Labeled C that accumulates in the light period in transitory C reserves like starch provides an internal source of label during the night.

A key feature is our use of parallel information about enrichment in free amino acids and enrichment in amino acid residues in protein to calculate the absolute rate of protein synthesis. In principle, data for each amino acid could be used separately to provide many parallel estimates of the rate of protein synthesis. However, most amino acids show complex labeling kinetics, with a slow and incomplete increase in enrichment in the light, a partial decrease in enrichment at night during the pulse, and a slow decline in enrichment during the chase (Fig. 1). While the reasons probably vary from case to case, some general features can be distinguished.

The most rapidly and completely labeled amino acids were Ala, Asp, Gly, and Ser. Ala and Asp are formed via reversible reactions from metabolites in central metabolism, and Gly and Ser are intermediates in the photorespiration pathway.

Most other amino acids are synthesized via long dedicated pathways, which may contribute to their slow labeling kinetics. The aromatic amino acids showed quite rapid labeling kinetics. This may be explained by two factors: first, the immediate precursors for the shikimate pathway are the Calvin-Benson cycle intermediate erythrose 4-phosphate and pyruvate, and both show rapid increases in enrichment during a pulse (Szecowka et al., 2013); and, second, flux through the shikimate pathway will be higher than in other amino acid biosynthesis pathways, because the shikimate pathway also provides precursors for phenylpropanoid metabolism. Their labeling was nevertheless slower than for Ala, Asp, Gly, and Ser.

Labeling kinetics are also complicated by the presence of multiple pools with different labeling kinetics. Many amino acids are located in both the cytoplasm and the vacuole (Riens et al., 1991; Weiner and Heldt, 1992; Winter et al., 1992; Krueger et al., 2011; Arrivault et al., 2014), and it is likely that the cytoplasmic pool is more rapidly labeled than the vacuolar pool (Szecowka et al., 2013). There may also be pools in nonphotosynthetic cells that are not rapidly labeled with $^{13}CO_2$. As a consequence, for many amino acids, the average enrichment may underestimate the enrichment in the precursor pool for protein synthesis.

Compartmentation may also contribute to the general decrease in average enrichment of free amino acids at night. Amino acid levels increase in the light and decrease at night, when they are used for protein synthesis (Gibon et al., 2009; Piques et al., 2009; Pal et al., 2013). The pools that are formed from newly fixed $^{13}CO_2$ in light are probably preferentially utilized at night, resulting in an increase in the contribution of unlabeled or weakly labeled pools at dawn. This is probably the reason for the large decrease in the enrichment of Gly at dawn. Gly undergoes especially large diurnal changes, due to its accumulation during photorespiration. The pool that is involved in photorespiration will be highly enriched (Szecowka et al., 2013). The large decrease in enrichment at dawn would be explained if there is another small and weakly labeled pool of Gly, which is compartmented from the pool that is involved in photorespiration. This weakly labeled pool would make little contribution to total Gly at dusk but a large contribution at dawn.

Incomplete labeling of free amino acid pools could also result from protein degradation, which will recycle unlabeled amino acids. However, turnover is generally quite low, so this is probably only a major factor in special cases, such as the *pgm* mutant at night.

In some cases, the slow labeling kinetic reflects specific features of metabolic pathways. One example is the unexpectedly slow labeling of Glu and Gln in the light (Fig. 1). This resembles an earlier observation that enrichment in Glu remains high during the first light

Table VI. *RGR and RGR^{STR} in Col-0 and the starchless pgm mutant*

Comparison of RGR^{STR} calculated from ^{13}C enrichment in the chase and RGR calculated from fresh weight and rosette area is shown. The data are for the same experiment as that of Table IV. The original data are provided in Supplemental Data Set S5.

Plant	RGR^{STR}	RGR
	STR d^{-1}	*mg mg^{-1} d^{-1}*
Col-0	0.205	0.221
pgm	0.127	0.137

period of a chase when Arabidopsis plants are labeled for several days with $^{13}CO_2$ and then chased with CO_2 (Huege et al., 2007). It has been known for some time that citrate levels fall in the light and recover at night (Scheible et al., 2000; Urbanczyk-Wochniak et al., 2005). It was recently reported that 2-oxoglutarate is labeled only slowly in the light (Szecowka et al., 2013) and that most of the Glu formed in the light derives from a preexisting and thus unlabeled pool of citrate (Tcherkez et al., 2012a, 2012b). Our data confirm that there is strong restriction on the flux of newly fixed ^{13}C to citrate, Glu, and Gln in the light and show that this restriction is relieved at night (Supplemental Fig. S1). This is presumably due either to inhibition in the light of pyruvate dehydrogenase activity (Tovar-Méndez et al., 2003) or of succinate dehydrogenase and fumarase by the mitochondrial thioredoxin system (Daloso et al., 2015).

Comparison of the labeling kinetics after supplying $^{13}CO_2$ to soil-grown plants and after supplying ^2H_2O to seedlings (Yang et al., 2010) reveals a qualitatively similar response for most amino acids. In both studies, Ala, Asp, Ser, and Gly labeled rapidly and reached high enrichment, while most minor amino acids labeled slowly and incompletely or showed biphasic kinetics, pointing to the presence of multiple pools. Ala and Asp labeled from ^2H_2O with half-times on the order of 0.5 to 0.7 h. In our study, half-times cannot be estimated, because the first sampling time point was at 4 h. However, by this time, maximum enrichment had been reached, indicating that the rate of labeling is not much slower than with ^2H_2O. This conclusion is supported by the rapid labeling of Ala reported by Szecowka et al. (2013). However, there were some differences between the labeling kinetics in our study and that of Yang et al. (2010). First, Ala and Asp labeled even more completely from ^2H_2O in seedlings than from $^{13}CO_2$ in soil-grown plants. Second, relative to other amino acids, Gly and Ser labeled more slowly from ^2H_2O in seedlings (compared with Ala and Asp, the half-times of Gly and Ser were about 5 and 3 times slower, respectively) than from $^{13}CO_2$ (labeling was not noticeably slower than for Ala and Asp; Szecowka et al., 2013). Third, Glu labeled much more rapidly from ^2H_2O in seedlings than from $^{13}CO_2$ in soil-grown plants. These differences may be due in part to different pool sizes and compartmentation in seedlings and older plants. They may also reflect a lower contribution of photosynthesis in the seedling system. A significant part of the seedling is nonphotosynthetic tissue, and their leaves were submerged, which is likely to reduce CO_2 access and the rate of photosynthesis. This might explain why, despite the ^2H_2O labeling of seedlings being performed in the light, labeling of Gly and Ser was relatively slow and labeling of Glu was much faster than in our experiments. It is also noteworthy that Yang et al. (2010) showed that the labeling kinetics of Ala and Asp are more than 50-fold slower from $^{15}NO_3$ than from ^2H_2O. Overall, the study of Yang et al. (2010) and our study show that most individual amino acids have complex and incomplete labeling patterns and underline the importance of taking this into account in any study of the rate of protein synthesis.

The reason for the complex labeling pattern of free amino acids will affect how this information should be used to calculate the rate of protein synthesis. For example, if low enrichment is due to the presence of multiple pools, use of the average value will result in overestimation of the rate of protein synthesis, because average enrichment will underestimate enrichment in the precursor pool. For this reason, we decided to use Ala, which showed the most rapid and complete labeling kinetics. The rate of protein synthesis will be slightly overestimated if the incomplete labeling of Ala is due to a separate unlabeled pool that is not involved in protein synthesis. However, analysis of the isotopomer labeling kinetics did not reveal any evidence for a small unlabeled pool of Ala. Any error introduced by the correction will be small anyway, because the overall enrichment in free Ala is high (typically, 80% in the light and 70% in the dark). Furthermore, our published analyses indicate that enrichment of Calvin-Benson cycle intermediates does not rise above 90%, presumably due to continual recycling of unlabeled C (Szecowka et al., 2013). In tissues or treatments where no amino acid shows a suitable enrichment pattern, it will be necessary to analyze the reasons for the incomplete enrichment in more detail to decide how to apply the correction.

Other small errors can arise in our simple protocol. One is that we did not measure the precise rate at which ^{13}C enrichment increased in Ala at the start of the pulse. Data from Szecowka et al. (2013) indicate that this occurs within 1 h even when labeling commences in the middle of the light period in the presence of a large unlabeled pool of Ala. Therefore, it is possible that our protocol results in a small but systematic underestimation of the rate of protein synthesis in the light. Another potential source of error is that some protein synthesis may occur in cell types that are not being labeled in the time frame of the $^{13}CO_2$ pulse. The observation that Ala showed similar enrichment in very young leaves and in mature leaves (Fig. 2C) argues against this being a general problem, but we cannot exclude the possibility that some specific cell types are missing from our analysis. Our calculation will also underestimate the rate of protein synthesis in conditions where rapid protein degradation recycles substantial amounts of label out of protein; however, in our experiments, this error is negligible, because the protein pool was only labeled up to about 25% and the rate of protein degradation was low in almost all investigated conditions.

It was necessary to perform pulse and chase experiments for a fairly long time, due to the relatively low rate of protein synthesis. Long pulses are also needed to analyze protein synthesis throughout the light/dark cycle. During this time, metabolism is moving through a series of quasisteady states. Our approach, which

involves comparison of a single precursor pool and a single product, can be applied to nonsteady-state conditions. While there are more sophisticated computational methods that analyze dynamic labeling patterns in large metabolic networks, they can only be applied when the metabolism is in steady state (Antoniewicz et al., 2006; Yuan et al., 2006, 2008; Young et al., 2011) and, in higher plants, also require assumptions about the spatial compartmentation (Szecowka et al., 2013; Heise et al., 2014; Ma et al., 2014). Although recent theoretical developments allow the analysis of dynamic labeling in metabolic nonsteady state in microbes (Antoniewicz, 2013), it remains challenging to apply these methods in higher plants.

While small errors will not greatly affect estimates of protein synthesis rates, they will affect the estimates of protein degradation rates. The latter are estimated from the difference between the rate of protein synthesis and the rate of growth. The rate of protein synthesis is often only slightly higher than the rate of growth, making our estimates of the rate of protein degradation sensitive to experimental and computational error.

Measurement of Plant Growth Rate

Estimation of the rate of protein degradation requires information about the growth rate. RGR was estimated by destructive harvesting of batches of plants during the pulse and chase. These values were confirmed by repeating these measurements in biologically replicated experiments with separately grown batches of plants in the same growth conditions (Supplemental Fig. S5C) and by time-series imaging of the leaf area of individual plants during the labeling experiments.

However, changes in plant size may not always reflect changes in biomass, defined as structural dry mass. They will differ, for example, when vacuole expansion is leading to a change in plant size that is not tightly coupled to changes in structural biomass. Therefore, we explored whether the $^{13}CO_2$ labeling could be used to monitor the enrichment of Glc in cell wall material and, hence, the rate of cell wall synthesis (Tables V and VI; Supplemental Data S5). This approach gave estimates of growth rate that agreed well with those obtained by measurements of plant size. It should be noted that this conclusion holds for an entire 24-h cycle but does not exclude the possibility that there may be temporal uncoupling of cell wall synthesis and increases in plant size at some times during the 24-h cycle (see below). A related problem will arise if expansion growth or other factors lead to a change in protein content during the experiment. In such cases, it is important to measure protein content and integrate this information into the calculation of protein degradation, as illustrated by the inclusion of information about changes in protein content in our analysis of the flux to growth and the rate of protein degradation in young leaves (Fig. 3)

Rates of Protein Synthesis and Degradation during a Diurnal Cycle

Our analysis reveals, for Arabidopsis Col-0 growing in short photoperiods, that the rate of protein synthesis in the light is about 3-fold higher than in the dark. This is a much larger decrease than for polysome loading, which only decreases by 25% to 30% (Pal et al., 2013; Sulpice et al., 2014). This comparison emphasizes that polysome loading only provides a qualitative proxy for the rate of protein synthesis. Several factors may lead to polysome loading underestimating the actual changes in the rate of protein synthesis, including changes in the rate of progression of ribosomes, ribosome stalling, or the presence of RNA in other high-mass structures.

As the plants were growing in an 8-h photoperiod, the amount of protein synthesized at night was about 40% of the total protein synthesis in a 24-h cycle. Cell wall synthesis also continues in the night at about one-third of the rate in the light, which is equivalent to about 40% of the cell wall synthesis occurring at night. These results underline the importance of nocturnal metabolism for growth. In an 8-h photoperiod, Col-0 accumulates about 52% of the daily fixed C as starch and other metabolites to support respiration and growth at night (Sulpice et al., 2014), of which about 10% is respired, leaving about 40% for the synthesis of structural biomass.

The rate of growth was about 22% d^{-1} in Col-0 in our growth conditions. Most of the synthesized protein, therefore, represents flux to growth. The estimated rate of protein degradation was 3.1% to 3.5% d^{-1}, which is much lower than the flux to growth. A combination of dilution by growth and protein degradation results in a global protein half-life of 3.1 to 3.5 d. This is similar to that predicted for Arabidopsis rosettes using ribosome abundance and polysome loading to model the global rate of protein synthesis (Piques et al., 2009). Thus, our results validate this simple linear model, which used literature values for the rate of ribosome progression to link quantitative molecular data to whole-plant growth. Our estimates also lie in a similar range to those obtained in experimental studies of small sets of mitochondrial proteins in Arabidopsis cell cultures (Nelson et al., 2013) and Arabidopsis rosettes (Li et al., 2012) and a set of 508 proteins in barley leaves (Nelson et al., 2014b).

Inappropriate Regulation of C Allocation Has Major Consequences for Protein Synthesis and Degradation

Starch turnover buffers plants against the daily alternation of light and dark (Smith and Stitt, 2007; Stitt and Zeeman, 2012). We used the starchless *pgm* mutant to investigate the importance of starch for the rate and timing of protein synthesis and degradation. Protein synthesis in *pgm* occurred at a similar rate to wild-type plants in the light but was strongly inhibited in the dark. Nonetheless, even though *pgm* is severely C starved at night (Gibon et al., 2004b, 2006), some protein synthesis

continued; the rate of protein synthesis in *pgm* in the last 12 h of the night was 40% of that in Col-0 in the night and 14% of that in Col-0 and *pgm* in the light. C starvation leads to strong changes in transcription, including the induction of many genes (Price et al., 2004; Bläsing et al., 2005; Usadel et al., 2008). Some of the residual protein synthesis in the night in *pgm* might be related to the synthesis of proteins that are required for C starvation responses. In agreement, C starvation-related enzymes like Glu dehydrogenase show an increase in abundance in *pgm* (Gibon et al., 2004a). The composition of ribosomes changes in response to C starvation (Hummel et al., 2012), although it is not yet known if this occurs rapidly enough to contribute to translational responses during the night in the *pgm* mutant.

The inhibition of cell wall synthesis at night in *pgm* was stronger than the inhibition of protein synthesis. This is consistent with the idea that the residual protein synthesis may be related to adjustment to low C, rather than growth. The partial inhibition of cell wall synthesis in the night in wild-type Col-0 and the complete inhibition in *pgm* underlines that the synthesis of cellulose, and probably other cell wall components, is tightly regulated by C.

Whereas amino acid levels decline during the night in wild-type Arabidopsis (Gibon et al., 2009; Pal et al., 2013; Sulpice et al., 2014), they increase in the *pgm* mutant (Gibon et al., 2006; Izumi et al., 2013), indicating that protein degradation is increased to provide amino acids as an alternative substrate for respiration. Our measurements provide direct evidence that protein degradation is increased at night in the *pgm* mutant. First, calculated rates of protein degradation are almost 2-fold higher in *pgm* than in wild-type plants. Second, there is a dramatic decrease in enrichment in almost all free amino acids at night in *pgm*, as expected if increased protein degradation is leading to rapid recycling of unlabeled amino acids. The only exception was Asn. C starvation leads to a strong increase in *ASN1* transcript abundance (Lam et al., 1996, 1998; Bläsing et al., 2005; Usadel et al., 2008). The level of Asn typically increases strongly in C-starved plants, providing a store for amino acid residues that are recycled from respired amino acids (Brouquisse et al., 1991; Lam et al., 1996; Gibon et al., 2006). The increase in Asn enrichment during the night in *pgm*, at a time when enrichment in all other amino acids is falling, provides evidence for the synthesis of Asn from prelabeled C pools, which may include Asp and organic acids like malate and fumarate.

The *pgm* mutant has an approximately 40% smaller daily net increment in protein than wild-type Col-0 (11.9%–13.7% d^{-1} in *pgm* compared with 20.5%–22.1% d^{-1} in Col-0). This closely matches the observed decrease in growth (38%) estimated either from size measurements or from Glc incorporation into the cell wall. This decrease in net protein synthesis is the result of a 29% reduction in the amount of protein synthesized per 24-h cycle, due to the lower rate of protein synthesis in the night, and a 26% to 35% increase in the rate of protein degradation (Table III). The decrease in growth-related protein synthesis may be even larger, because some of the protein synthesis at night in *pgm* may serve to produce proteins that are involved in C starvation responses (see above). Furthermore, this daily alternation between net protein synthesis and degradation results in a time offset and wasteful futile cycle in *pgm*, in which energy is used to synthesize proteins in the light period that are degraded in the dark. The low rate of protein synthesis during the night and the daily cycle of protein synthesis and degradation will also result in less efficient use of the translational apparatus in *pgm* than in wild-type Col-0. Many explanations have been advanced for the poor growth of *pgm* in short photoperiods, ranging from loss of C due to rapid respiration as sugars decline from high to low levels at the start of the night (Caspar et al., 1985) to disturbances in root metabolism (Brauner et al., 2014). However, they do not provide a quantitative explanation for the growth inhibition; indeed, the increase in respiration accounts for only a small proportion of the assimilated C. Furthermore, some of these effects may be secondary; for example, the high rate of respiration in the first part of the night can be at least partly explained as a consequence of the continuation of protein and cell wall synthesis at this time in the *pgm* mutant, rather than as wasteful stimulation of respiration by high sugar.

Changes in Temperature Do Not Have a Major Impact on Protein Degradation

High temperature results in an increase in respiration, in particular maintenance respiration, (Penning de Vries et al., 1979; Amthor, 2000). In Arabidopsis, maintenance respiration doubles between growth temperatures of 16°C and 24°C (Pyl et al., 2012). The major maintenance costs are thought to be protein turnover and the maintenance of gradients across membranes (Penning de Vries, 1975; Amthor, 2000). Our results show that increasing the growth temperature from 20°C to 28°C leads to a parallel 30% increase in both the rate of protein synthesis and the rate of protein degradation. This indicates that, although an increase in protein turnover could contribute to the rise in maintenance respiration at high temperature, it is unlikely to be the only factor. Two other recent studies also indicate that protein turnover is not the main factor underlying the increase in maintenance respiration at high temperature. Pilkington et al. (2015) estimated that the ATP provided by maintenance respiration in Arabidopsis growing in a short photoperiod would support the synthesis and degradation of 4% of the total protein per h, which is 10-fold higher than the measured rate of protein degradation. Cheung et al. (2013) used metabolic flux balance analysis to estimate the rate of consumption of ATP and NADPH during maintenance in Arabidopsis cell

cultures and concluded that up to one-third of the output of maintenance respiration was NADPH, which is presumably used for processes other than protein synthesis.

Darkness Does Not Lead to a Preferential Inhibition of all Protein Synthesis in the Plastid

Although our protocol was designed to analyze global protein synthesis, we were interested to learn if it could be modified to investigate individual proteins. Using a procedure adapted from Allen et al. (2012), we found that synthesis of the plastid-encoded RBCL continues in the dark, being inhibited to approximately the same extent as the synthesis of the nucleus-encoded RBCS and the overall rate of protein synthesis. This was initially surprising, as it is thought that plastid translation is inhibited in the dark (Marín-Navarro et al., 2007). This idea is based on studies of protein synthesis in isolated chloroplasts and on studies of plastid-encoded proteins that are targeted to the thylakoids. However, isolated chloroplasts may not be a perfect model for studying plastid protein synthesis in whole leaves. It is also possible that the synthesis of a soluble protein like RBCL may be differently regulated from proteins that are assembled into protein complexes in the thylakoid membrane and whose targeting and assembly may be light dependent (Keegstra and Cline, 1999; Cline and Dabney-Smith, 2008). Furthermore, as Rubisco represents up to 40% of total leaf protein (Eckardt et al., 1997), restricting its synthesis to the light period would severely restrict the availability of ribosomes for the synthesis of other protein species.

The question arises of whether our approach can be adapted to analyze the synthesis and degradation of less abundant proteins. One possibility might be to combine it with the approach used by Yang et al. (2010), who overexpressed tagged variants of selected proteins to aid their purification. This approach will probably be limited by the sensitivity of the detection of amino acids in gas chromatography-mass spectrometry. Alternatively, ^{13}C-labeled protein might be converted to peptides for analysis, as was done by Yang et al. (2010). In this case, the major challenges will be deconvolution of the complex envelope and correction of the enrichment for all amino acids in the peptide, including many with very incomplete enrichment in the precursor free amino acid pool. These challenges are shared by strategies using $^{2}H_2O$ labeling. While the peptide envelope is simpler when ^{15}N is used as a label (Li et al., 2012; Nelson et al., 2014a, 2014b), the slow labeling kinetic of amino acids in higher plants (Yang et al., 2010) means that this approach is probably unsuited for rapidly turning over proteins. The decision between labeling with $^{13}CO_2$ and $^{2}H_2O$ may depend on the tissue and condition under investigation, as this will affect which isotope can be introduced with the least disturbance, the extent to which inhibitory effects of $^{2}H_2O$ can be minimized, and the speed and completeness of the labeling kinetics of free amino acid pools.

In conclusion, we have developed a relatively simple method that introduces label via photosynthetic CO_2 fixation and provides quantitative information on the global rate of protein synthesis and degradation. The key feature is parallel determination of isotope enrichment in the products and in the metabolite precursors from which they are synthesized. We have applied this approach to investigate the relationship between protein metabolism, the plant energy budget and growth, and the impact of development and environmental perturbations on protein synthesis and degradation. While it can also be used to study individual proteins, this application will probably be restricted to abundant proteins. We have shown that the approach can be extended to provide quantitative information about the rate of cell wall synthesis and expect that it will also be applicable to other classes of structural components as well as specialized metabolites. This would allow a comprehensive analysis of the rates of synthesis of all major structural components in the plant as well as major defense metabolites. An equally important challenge will be to adapt this approach to introduce $^{13}CO_2$ via photosynthesis, allow label to move through the plant via endogenous transport routes, and analyze fluxes to growth in nonphotosynthetic organs such as roots and seeds.

MATERIALS AND METHODS

Plant Growth Conditions

Arabidopsis (*Arabidopsis thaliana*) Col-0 seeds were germinated and grown in soil for 1 week with 16 h of light (20°C in the light and 6°C at night, 150 μmol m^{-2} s^{-1} fluorescent light, and 60%–70% relative humidity) before transfer to short days (8 h of light, 150 μmol m^{-2} s^{-1}, 20°C/19°C in the light and dark, and 60%–70% relative humidity). Fourteen days after sowing, five seedlings were pricked into 10-cm pots and grown under the same conditions in a controlled-environment chamber (model E-36L; Percival Scientific; Thimm et al., 2004). In some experiments, Col-0 plants were transferred to short days with 28°C/28°C in the light and dark (8 h of light, 150 μmol m^{-2} s^{-1}, and 60%–70% relative humidity) at 18 d after sowing and used for the labeling experiment at 21 d after sowing. The *pgm* mutant was germinated as above and grown in a 12-h photoperiod (20°C/19°C in the light and dark, 150 μmol m^{-2} s^{-1} fluorescent light, and 60%–70% relative humidity) until 25 d after sowing and then shifted to an 8-h photoperiod 3 d prior to the experiment at 28 d after sowing.

$^{13}CO_2$ Feeding Experiments

$^{13}CO_2$ feeding was carried in a Plexiglas box (internal dimensions, 60 × 31 × 17.4 cm, holding up to 17 10-cm pots, each containing five plants) in a Percival controlled-environment chamber. Three-week-old plants were transferred to the chamber 3 d before the experiment. The labeling chamber was supplied with a premixed air stream containing 450 μL L^{-1} CO_2 or $^{13}CO_2$, 21% (v/v) oxygen, and 79% (v/v) nitrogen. At a flow rate of 5 L min^{-1}, the air in the chamber was completely replaced in 20 min. During $^{13}CO_2$ feeding, the air exiting the box was passed through a gas-wash bottle filled with soda lime pellets with indicator (Merck Millipore) to prevent the release of $^{13}CO_2$ into the growth chamber. Unless specified, $^{13}CO_2$ feeding was performed in growth conditions with photon flux density and temperature inside the box of approximately 150 μmol m^{-2} s^{-1} and 20°C/18°C in light and dark, respectively. Labeling started 1 h before dawn and was continued through an entire light and dark period. Plants were harvested by opening the lid of the labeling chamber, removing the plants and submerging them in liquid N_2, and

reclosing the lid within 10 s. Immediately following harvest, leaf tissues were frozen in liquid nitrogen. Samples were ground to a fine powder at −70°C using a cryogenic grinding robot (http://www.labman.co.uk/portfolio-type/cryogenic-plant-grinder-and-dispensing-system/; Labman Automation) and stored until analysis at −80°C.

Metabolite and Protein Analysis

Homogenized frozen plant material (30 mg) was extracted with methanol followed by phase separation using chloroform-water as described by Heise et al. (2014). Ice-cold 100% (v/v) methanol and ribitol (1.31 mM) solution as an internal quantitative standard were added to the homogenized plant material and incubated for 10 min at 70°C. After the incubation, the samples were centrifuged. The pellet was kept for protein and cell wall analysis. The supernatant was used for phase separation using chloroform-water. The apolar (chloroform) phase was discarded. The upper polar phase was used for methoxysilylation of metabolites with *N*-methyl-*N*-trimethylsilyltrifluoroacetamide followed by GC-TOF-MS analysis using the same conditions and settings as described by Lisec et al. (2006). Total protein was extracted from the pellet using 6 M urea/2 M thiourea solution. Total protein was measured as described by Bradford (1976). Protein (about 50 μg) was precipitated with 15% (v/v) ice-cold TCA and washed with ice-cold 100% (v/v) acetone. The pellet was chemically hydrolyzed with 6 M hydrochloric acid at 100°C for 24 h at atmospheric pressure (Williams et al., 2010). The hydrolysate was dried and derivatized with *N*-methyl-*N*-trimethylsilyltrifluoroacetamide for GC-TOF-MS. The resulting chromatograms were processed as described by Heise et al. (2014). Briefly, chromatography peaks were manually assigned to parent metabolites, and ion intensity was determined using TagFinder (Luedemann et al., 2008) based on mass spectra and retention indices in a reference library derived from the Golm Metabolome Database (http://gmd.mpimp-golm.mpg.de; Kopka et al., 2005). Using the CORRECTOR software tool (Heuge et al., 2014), mass fragment intensities were adjusted to correct for the presence of naturally occurring stable isotopes. Fragmental isotope enrichment was calculated according to Equation 1:

$$\text{enrichment } (\%) = \frac{\sum_{n=0}^{i}(n \times m_n)}{n \times \sum_{n=0}^{i} m_n} \times 100 \quad (1)$$

where n represents the number of ^{13}C atoms in the detected fragment, and m_n is the corrected intensity of a mass fragment that contains n ^{13}C atoms. In addition, relative isotope abundance (RIA) for each metabolite was calculated by following Equation 2:

$$\text{RIA } (\%) = \frac{m_n}{\sum_{n=0}^{i} m_n} \times 100 \quad (2)$$

Signal intensity was high enough to quantify the ^{13}C enrichment in Glu, Asp, Ala, Ser, Gly, Ile, Val, Lys, Phe, Tyr, and Pro, but other amino acids could not be analyzed due to low abundance.

Cell Wall Analysis

The pellet remaining after protein extraction was used for cell wall analysis as described by Saeman et al. (1945) with modifications. After removing the urea/thiourea solution from the pellet by washing five times with distilled water, the pellet was resuspended in 0.3 mL of 0.1 M acetate/NaOH (pH 4.9). Starch in the pellet was removed in two sequential 16-h digestions with 0.2 mL of starch degradation mix (16.8 units mL^{-1} amyloglucosidase and 30 units mL^{-1} α-amylase) at 37°C. The remaining pellet was thoroughly washed three times by mixing it with 0.5 mL of distilled water. The sample was then incubated in 72% (v/v) sulfuric acid in 2-mL screw-cap microcentrifuge tubes at room temperature for 1 h, water was added to the sample to adjust sulfuric acid to 1 M, and incubation was continued for 3 h at 100°C to hydrolyze polysaccharides including cellulose. The hydolysate was neutralized with 1 mL of 20% (v/v) *N*,*N*-dioctylamine, and excess *N*,*N*-dioctylamine was then removed from the aqueous phase by washing three times with 1 mL of 100% (v/v) chloroform. The hydrolysate was dried and stored at −80°C until subsequent derivatization for GC-TOF-MS analysis to quantify ^{13}C enrichment in Glc.

Determination of Enrichment in RBCL and RBCS

RBCL and RBCS were isolated from total protein and analyzed for ^{13}C enrichment as described by Allen et al. (2012) with modifications. Protein was separated on 15% (v/v) SDS-PAGE Tris-HCl gels (PowerPac Universal Supply; Bio-Rad). The gel was electroblotted to a Bio-Rad immunoblot polyvinylidene difluoride membrane and stained with Ponceaus S solution (Sigma-Aldrich). Using M_r markers, RBCL and RBCS bands were located, excised from the membrane, and destained. Protein amino acids were hydrolyzed on the membrane overnight with 6 M hydrochloric acid at 110°C. The hydrolysate was dried and stored at −80°C until subsequent derivatization for GC-TOF-MS analysis.

RGR

The RGR of rosette biomass (mg mg^{-1} d^{-1}) was determined by estimating the slope of the natural logarithm-transformed plant weight measured for at least 3 d consecutively during the experiment (Hoffmann and Poorter, 2002). RGR from the rosette leaf area (mm^2 mm^{-2} d^{-1}) was estimated from images acquired using a Canon PowerShot SX500 IS digital camera. Area was extracted from the images using Adobe Photoshop CS5.

Estimation of the Change in Protein Content per Day in Young Growing Leaves

Calculation of the rate of protein degradation in young growing leaves (Fig. 3) required information about the rate at which the protein content decreased due to the relatively large technical error in measuring protein and the limited material in young leaf samples; this could not be accurately determined in the samples used for ^{13}C enrichment analysis. In parallel experiments, Arabidopsis Col-0 was grown in identical conditions, and after 21 d, sequential leaves were pooled from 60 plants, and leaf area and protein were determined from three biological replicates (Supplemental Table S3, worksheet leaf protein calculation). The rate of leaf initiation (0.41 leaves d^{-1}) was determined in the same material, allowing the data for leaf area and protein content for each leaf to be plotted on a time scale. These plots were inspected to determine the change in protein content per day: $\Delta P_i = (p_i - p_{i+1})/p_i$, where ΔP_i is the decrease in protein per day in leaf i and p_i and p_{i+1} are the leaf protein content in leaf i and the protein content of leaf i the next day, respectively. The protein required per day for growth was calculated as $LRGR_i \times (1 - \Delta P_i)$, where $LRGRi$ is the LRGR in leaf i obtained from sequential images of the rosettes from 10 plants.

Supplemental Data

The following supplemental materials are available.

Supplemental Figure S1. Enrichment kinetics of organic acids in Col-0 growing in an 8-h photoperiod.

Supplemental Figure S2. Labeling kinetics for all detected isotopomers of the free amino acid pools in a pulse and chase in Col-0 growing in an 8-h photoperiod.

Supplemental Figure S3. Comparison of enrichment in the free amino acid pool with the rate of incorporation of label into the corresponding amino acid residue in protein.

Supplemental Figure S4. Comparison of the ^{13}C washout curve for different amino acid residues in protein during the chase.

Supplemental Figure S5. Determination of the RGR of Col-0 growing in an 8-h photoperiod.

Supplemental Figure S6. Kinetics of changes in enrichment in free amino acids during a 24-h pulse in wild-type Col-0 and the starchless *pgm* mutant growing in an 8-h photoperiod.

Supplemental Table S1. Enrichment in free amino acids, other metabolites, and amino acids in protein in Col-0 growing in an 8-h photoperiod.

Supplemental Table S2. Changes in the levels of amino acids and other metabolites between dawn and dusk in Col-0 growing in an 8-h photoperiod.

Supplemental Table S3. Protein synthesis and degradation rates estimated at different growth stages of leaf development.

Supplemental Table S4. Enrichment in free amino acids, other metabolites, and amino acids in protein in Col-0 and the starchless mutant *pgm* growing in an 8-h photoperiod.

Supplemental Data Set S1. Col-0 growing in an 8-h photoperiod at 20°C.

Supplemental Data Set S2. Six stages of leaf development in Col-0 growing in an 8-h photoperiod at 20°C.

Supplemental Data Set S3. Col-0 growing in an 8-h photoperiod at 20°C and 28°C.

Supplemental Data Set S4. Enrichment in RBCL and RBCS in the light and dark in Col-0 growing in an 8-h photoperiod at 20°C.

Supplemental Data Set S5. Col-0 and the starchless *pgm* mutant growing in an 8-h photoperiod at 20°C.

ACKNOWLEDGMENTS

We thank Christin Abel for help and Stéphanie Arrivault, John E. Lunn, Roosa A.E. Laitinen, and Carlos Figueroa for discussions.

Received February 11, 2015; accepted March 25, 2015; published March 25, 2015.

LITERATURE CITED

Allen DK, Laclair RW, Ohlrogge JB, Shachar-Hill Y (2012) Isotope labelling of Rubisco subunits provides in vivo information on subcellular biosynthesis and exchange of amino acids between compartments. Plant Cell Environ **35:** 1232–1244

Amthor JS (2000) The McCree-de Wit-Penning de Vries-Thornley respiration paradigms: 30 years later. Ann Bot (Lond) **86:** 1–20

Antoniewicz MR (2013) Dynamic metabolic flux analysis: tools for probing transient states of metabolic networks. Curr Opin Biotechnol **24:** 973–978

Antoniewicz MR, Kelleher JK, Stephanopoulos G (2006) Determination of confidence intervals of metabolic fluxes estimated from stable isotope measurements. Metab Eng **8:** 324–337

Araújo WL, Tohge T, Ishizaki K, Leaver CJ, Fernie AR (2011) Protein degradation: an alternative respiratory substrate for stressed plants. Trends Plant Sci **16:** 489–498

Arrivault S, Guenther M, Florian A, Encke B, Feil R, Vosloh D, Lunn JE, Sulpice R, Fernie AR, Stitt M, et al (2014) Dissecting the subcellular compartmentation of proteins and metabolites in Arabidopsis leaves using non-aqueous fractionation. Mol Cell Proteomics **13:** 2246–2259

Bailey-Serres J (1999) Selective translation of cytoplasmic mRNAs in plants. Trends Plant Sci **4:** 142–148

Barneix AJ, Cooper HD, Stulen I, Lambers H (1988) Metabolism and translocation of nitrogen in two *Lolium perenne* populations with contrasting rates of mature leaf respiration and yield. Physiol Plant **72:** 631–636

Beilharz TH, Preiss T (2004) Translational profiling: the genome-wide measure of the nascent proteome. Brief Funct Genomics Proteomics **3:** 103–111

Bläsing OE, Gibon Y, Günther M, Höhne M, Morcuende R, Osuna D, Thimm O, Usadel B, Scheible WR, Stitt M (2005) Sugars and circadian regulation make major contributions to the global regulation of diurnal gene expression in *Arabidopsis*. Plant Cell **17:** 3257–3281

Bouma TJ, De Visser R, Janssen JHJA, De Kock MJ, Van Leeuwen PH, Lambers H (1994) Respiratory energy requirements and rate of protein turnover in vivo determined by the use of an inhibitor of protein synthesis and a probe to assess its effect. Physiol Plant **92:** 585–594

Bradford MM (1976) A rapid and sensitive method for the quantitation of microgram quantities of protein utilizing the principle of protein-dye binding. Anal Biochem **72:** 248–254

Branco-Price C, Kaiser KA, Jang CJ, Larive CK, Bailey-Serres J (2008) Selective mRNA translation coordinates energetic and metabolic adjustments to cellular oxygen deprivation and reoxygenation in Arabidopsis thaliana. Plant J **56:** 743–755

Branco-Price C, Kawaguchi R, Ferreira RB, Bailey-Serres J (2005) Genome-wide analysis of transcript abundance and translation in Arabidopsis seedlings subjected to oxygen deprivation. Ann Bot (Lond) **96:** 647–660

Brauner K, Hörmiller I, Nägele T, Heyer AG (2014) Exaggerated root respiration accounts for growth retardation in a starchless mutant of *Arabidopsis thaliana*. Plant J **79:** 82–91

Brouquisse R, James F, Raymond P, Pradet A (1991) Study of glucose starvation in excised maize root tips. Plant Physiol **96:** 619–626

Buse MG, Reid SS (1975) Leucine: a possible regulator of protein turnover in muscle. J Clin Invest **56:** 1250–1261

Caspar T, Huber SC, Somerville CR (1985) Alterations in growth, photosynthesis, and respiration in a starchless mutant of *Arabidopsis thaliana* (L.) deficient in chloroplast phosphoglucomutase activity. Plant Physiol **79:** 11–17

Chen WP, Yang XY, Harms GL, Gray WM, Hegeman AD, Cohen JD (2011) An automated growth enclosure for metabolic labeling of *Arabidopsis thaliana* with ^{13}C-carbon dioxide: an in vivo labeling system for proteomics and metabolomics research. Proteome Sci **9:** 9

Cheung CY, Williams TC, Poolman MG, Fell DA, Ratcliffe RG, Sweetlove LJ (2013) A method for accounting for maintenance costs in flux balance analysis improves the prediction of plant cell metabolic phenotypes under stress conditions. Plant J **75:** 1050–1061

Cline K, Dabney-Smith C (2008) Plastid protein import and sorting: different paths to the same compartments. Curr Opin Plant Biol **11:** 585–592

Daloso DM, Müller K, Obata T, Florian A, Tohge T, Bottcher A, Riondet C, Bariat L, Carrari F, Nunes-Nesi A, et al (2015) Thioredoxin, a master regulator of the tricarboxylic acid cycle in plant mitochondria. Proc Natl Acad Sci USA **112:** E1392–E1400

Dean C, Leech RM (1982) Genome expression during normal leaf development: 1. Cellular and chloroplast numbers and DNA, RNA, and protein levels in tissues of different ages within a seven-day-old wheat leaf. Plant Physiol **69:** 904–910

Detchon P, Possingham JV (1972) Ribosomal-RNA distribution during leaf development in spinach. Phytochemistry **11:** 943–947

Dungey NO, Davies DD (1982) Protein turnover in the attached leaves of non-stressed and stressed barley seedlings. Planta **154:** 435–440

Eckardt NA, Snyder GW, Portis AR Jr, Orgen WL (1997) Growth and photosynthesis under high and low irradiance of *Arabidopsis thaliana* antisense mutants with reduced ribulose-1,5-bisphosphate carboxylase/oxygenase activase content. Plant Physiol **113:** 575–586

Ferguson DL, Guikema JA, Paulsen GM (1990) Ubiquitin pool modulation and protein degradation in wheat roots during high temperature stress. Plant Physiol **92:** 740–746

Foyer CH, Parry M, Noctor G (2003) Markers and signals associated with nitrogen assimilation in higher plants. J Exp Bot **54:** 585–593

Fraser CM, Chapple C (2011) The phenylpropanoid pathway in Arabidopsis. The Arabidopsis Book **9:** e0152, doi/10.1199/tab0152

Fritz C, Matt P, Müller C, Feil R, Stitt M (2006) Impact of the carbon-nitrogen status on the amino acid profile in tobacco leaves. Plant Cell Environ **29:** 2055–2076

Galili G (2002) New insights into the regulation and functional significance of lysine metabolism in plants. Annu Rev Plant Biol **53:** 27–43

Gibon Y, Bläsing O, Hannemann J, Carillo P, Höhne M, Cross J, Selbig J, Stitt M (2004a) A robot-based platform to measure multiple enzyme activities in *Arabidopsis* using a set of cycling assays: comparison of changes of enzyme activities and transcript levels during diurnal cycles and in prolonged darkness. Plant Cell **16:** 3304–3325

Gibon Y, Bläsing OE, Palacios-Rojas N, Pankovic D, Hendriks JHM, Fisahn J, Höhne M, Günther M, Stitt M (2004b) Adjustment of diurnal starch turnover to short days: depletion of sugar during the night leads to a temporary inhibition of carbohydrate utilization, accumulation of sugars and post-translational activation of ADP-glucose pyrophosphorylase in the following light period. Plant J **39:** 847–862

Gibon Y, Pyl ET, Sulpice R, Lunn JE, Höhne M, Günther M, Stitt M (2009) Adjustment of growth, starch turnover, protein content and central metabolism to a decrease of the carbon supply when Arabidopsis is grown in very short photoperiods. Plant Cell Environ **32:** 859–874

Gibon Y, Usadel B, Blaesing OE, Kamlage B, Hoehne M, Trethewey R, Stitt M (2006) Integration of metabolite with transcript and enzyme activity profiling during diurnal cycles in Arabidopsis rosettes. Genome Biol **7:** R76

Gruhler A, Schulze WX, Matthiesen R, Mann M, Jensen ON (2005) Stable isotope labeling of Arabidopsis thaliana cells and quantitative proteomics by mass spectrometry. Mol Cell Proteomics **4:** 1697–1709

He CY, Merrick BA, Mansfield BK, Hite MC, Daluge DR, Selkirk JK (1991) Comparison of ^{14}C-amino acid mixture and [^{35}S]methionine labeling of cellular proteins from mouse fibroblast C3H10T1/2 cells by two-dimensional gel electrophoresis. Electrophoresis **12:** 658–666

Heise R, Arrivault S, Szecowka M, Tohge T, Nunes-Nesi A, Stitt M, Nikoloski Z, Fernie AR (2014) Flux profiling of photosynthetic carbon metabolism in intact plants. Nat Protoc **9:** 1803–1824

Hoffmann WA, Poorter H (2002) Avoiding bias in calculations of relative growth rate. Ann Bot (Lond) **90:** 37–42

Hsiao TC (1970) Rapid changes in levels of polyribosomes in *Zea mays* in response to water stress. Plant Physiol **46:** 281–285

Huege J, Goetze J, Dethloff F, Junker B, Kopka J (2014) Quantification of stable isotope label in metabolites via mass spectrometry. Methods Mol Biol **1056:** 213–223

Huege J, Sulpice R, Gibon Y, Lisec J, Koehl K, Kopka J (2007) GC-EI-TOF-MS analysis of in vivo carbon-partitioning into soluble metabolite pools of higher plants by monitoring isotope dilution after $^{13}CO_2$ labelling. Phytochemistry **68:** 2258–2272

Huffaker RC, Peterson LW (1974) Protein turnover in plants and possible means of its regulation. Annu Rev Plant Physiol **25:** 363–392

Hummel M, Cordewener JHG, de Groot JCM, Smeekens S, America AHP, Hanson J (2012) Dynamic protein composition of Arabidopsis thaliana cytosolic ribosomes in response to sucrose feeding as revealed by label free MSE proteomics. Proteomics **12:** 1024–1038

Izumi M, Hidema J, Makino A, Ishida H (2013) Autophagy contributes to nighttime energy availability for growth in Arabidopsis. Plant Physiol **161:** 1682–1693

Kawaguchi R, Girke T, Bray EA, Bailey-Serres J (2004) Differential mRNA translation contributes to gene regulation under non-stress and dehydration stress conditions in *Arabidopsis thaliana*. Plant J **38:** 823–839

Kawaguchi R, Williams AJ, Bray EA, Bailey-Serres J (2003) Water-deficit induced translational control in *Nicotiana tabacum*. Plant Cell Environ **26:** 221–229

Keegstra K, Cline K (1999) Protein import and routing systems of chloroplasts. Plant Cell **11:** 557–570

Kopka J, Schauer N, Krueger S, Birkemeyer C, Usadel B, Bergmüller E, Dörmann P, Weckwerth W, Gibon Y, Stitt M, et al (2005) GMD@CSB. DB: the Golm Metabolome Database. Bioinformatics **21:** 1635–1638

Krueger S, Giavalisco P, Krall L, Steinhauser MC, Büssis D, Usadel B, Flügge UI, Fernie AR, Willmitzer L, Steinhauser D (2011) A topological map of the compartmentalized *Arabidopsis thaliana* leaf metabolome. PLoS ONE **6:** e17806

Kushner DJ, Baker A, Dunstall TG (1999) Pharmacological uses and perspectives of heavy water and deuterated compounds. Can J Physiol Pharmacol **77:** 79–88

Lam HM, Coschigano KT, Oliveira IC, Melo-Oliveira R, Coruzzi GM (1996) The molecular genetics of N assimilation into amino acids in higher plants. Annu Rev Plant Physiol Plant Mol Biol **47:** 569–593

Lam HM, Hsieh MH, Coruzzi G (1998) Reciprocal regulation of distinct asparagine synthetase genes by light and metabolites in *Arabidopsis thaliana*. Plant J **16:** 345–353

Lattanzi FA, Schnyder H, Thornton B (2005) The sources of carbon and nitrogen supplying leaf growth: assessment of the role of stores with compartmental models. Plant Physiol **137:** 383–395

Lehmeier CA, Wild M, Schnyder H (2013) Nitrogen stress affects the turnover and size of nitrogen pools supplying leaf growth in a grass. Plant Physiol **162:** 2095–2105

Li L, Nelson CJ, Solheim C, Whelan J, Millar AH (2012) Determining degradation and synthesis rates of Arabidopsis proteins using the kinetics of progressive ^{15}N labeling of two-dimensional gel-separated protein spots. Mol Cell Proteomics **11:** M111.010025

Lisec J, Schauer N, Kopka J, Willmitzer L, Fernie AR (2006) Gas chromatography mass spectrometry-based metabolite profiling in plants. Nat Protoc **1:** 387–396

Lodish H, Berk A, Zipursky SL, Matsudaira P, Baltimore D, Darnell J, editors (2011) The dynamic plant cell wall. *In* Molecular Cell Biology, Ed 4. WH Freeman, New York, section 22.5 http://www.ncbi.nlm.nih.gov/books/NBK21709/ (April 15, 2015)

Luedemann A, Strassburg K, Erban A, Kopka J (2008) TagFinder for the quantitative analysis of gas chromatography-mass spectrometry (GC-MS)-based metabolite profiling experiments. Bioinformatics **24:** 732–737

Ma F, Jazmin LJ, Young JD, Allen DK (2014) Isotopically nonstationary ^{13}C flux analysis of changes in *Arabidopsis thaliana* leaf metabolism due to high light acclimation. Proc Natl Acad Sci USA **111:** 16967–16972

Marín-Navarro J, Manuell AL, Wu J, P Mayfield S (2007) Chloroplast translation regulation. Photosynth Res **94:** 359–374

Martin SF, Munagapati VS, Salvo-Chirnside E, Kerr LE, Le Bihan T (2012) Proteome turnover in the green alga *Ostreococcus tauri* by time course ^{15}N metabolic labeling mass spectrometry. J Proteome Res **11:** 476–486

Masclaux-Daubresse C, Chardon F (2011) Exploring nitrogen remobilization for seed filling using natural variation in *Arabidopsis thaliana*. J Exp Bot **62:** 2131–2142

Mastrobuoni G, Irgang S, Pietzke M, Assmus HE, Wenzel M, Schulze WX, Kempa S (2012) Proteome dynamics and early salt stress response of the photosynthetic organism *Chlamydomonas reinhardtii*. BMC Genomics **13:** 215

Mitra R, Burton J, Varner JE (1976) Deuterium oxide as a tool for the study of amino acid metabolism. Anal Biochem **70:** 1–17

Nelson CJ, Alexova R, Jacoby RP, Millar AH (2014a) Proteins with high turnover rate in barley leaves estimated by proteome analysis combined with in planta isotope labeling. Plant Physiol **166:** 91–108

Nelson CJ, Li L, Jacoby RP, Millar AH (2013) Degradation rate of mitochondrial proteins in *Arabidopsis thaliana* cells. J Proteome Res **12:** 3449–3459

Nelson CJ, Li L, Millar AH (2014b) Quantitative analysis of protein turnover in plants. Proteomics **14:** 579–592

Nicolaï M, Roncato MA, Canoy AS, Rouquié D, Sarda X, Freyssinet G, Robaglia C (2006) Large-scale analysis of mRNA translation states during sucrose starvation in Arabidopsis cells identifies cell proliferation and chromatin structure as targets of translational control. Plant Physiol **141:** 663–673

Ong SE, Blagoev B, Kratchmarova I, Kristensen DB, Steen H, Pandey A, Mann M (2002) Stable isotope labeling by amino acids in cell culture, SILAC, as a simple and accurate approach to expression proteomics. Mol Cell Proteomics **1:** 376–386

Ong SE, Mann M (2006) A practical recipe for stable isotope labeling by amino acids in cell culture (SILAC). Nat Protoc **1:** 2650–2660

Pal SK, Liput M, Piques M, Ishihara H, Obata T, Martins MC, Sulpice R, van Dongen JT, Fernie AR, Yadav UP, et al (2013) Diurnal changes of polysome loading track sucrose content in the rosette of wild-type Arabidopsis and the starchless *pgm* mutant. Plant Physiol **162:** 1246–1265

Pannemans DL, Schaafsma G, Westerterp KR (1997) Calcium excretion, apparent calcium absorption and calcium balance in young and elderly subjects: influence of protein intake. Br J Nutr **77:** 721–729

Penning de Vries FWT (1975) The cost of maintenance processes in plant cells. Ann Bot (Lond) **39:** 77–92

Penning de Vries FWT, Brunsting AH, van Laar HH (1974) Products, requirements and efficiency of biosynthesis: a quantitative approach. J Theor Biol **45:** 339–377

Penning de Vries FWT, Witlage JM, Kremer D (1979) Rates of respiration and of increase in structural dry matter in young wheat, ryegrass and maize plants in relation to temperature, to water stress and to their sugar content. Ann Bot (Lond) **44:** 595–609

Pilkington SM, Encke B, Krohn N, Höhne M, Stitt M, Pyl ET (2015) Relationship between starch degradation and carbon demand for maintenance and growth in Arabidopsis thaliana in different irradiance and temperature regimes. Plant Cell Environ **38:** 157–171

Piques M, Schulze WX, Höhne M, Usadel B, Gibon Y, Rohwer J, Stitt M (2009) Ribosome and transcript copy numbers, polysome occupancy and enzyme dynamics in Arabidopsis. Mol Syst Biol **5:** 314

Pocrnjic Z, Mathews RW, Rappaport S, Haschemeyer AEV (1983) Quantitative protein synthetic rates in various tissues of a temperate fish in vivo by the method of phenylalanine swamping. Comp Biochem Physiol B **74:** 735–738

Pons T, van Rijnberk H, Scheurwater I, van der Werf A (1993) Importance of the gradient in photosynthetically active radiation in a vegetation stand for leaf nitrogen allocation in two monocotyledons. Oecologia **95:** 416–424

Poorter H, Nagel O (2000) The role of biomass allocation in the growth response of plants to different levels of light, CO_2, nutrients and water: a quantitative review. Aust J Plant Physiol **27:** 595–607

Price J, Laxmi A, St Martin SK, Jang JC (2004) Global transcription profiling reveals multiple sugar signal transduction mechanisms in *Arabidopsis*. Plant Cell **16:** 2128–2150

Pyl ET, Piques M, Ivakov A, Schulze W, Ishihara H, Stitt M, Sulpice R (2012) Metabolism and growth in *Arabidopsis* depend on the daytime temperature but are temperature-compensated against cool nights. Plant Cell **24:** 2443–2469

Rapparini F, Cohen J, Slovin J (1999) Indole-3-acetic acid biosynthesis in Lemna gibba studied using stable isotope labeled anthranilate and tryptophan. Plant Growth Regul **27:** 139–144

Riens B, Lohaus G, Heineke D, Heldt HW (1991) Amino acid and sucrose content determined in the cytosolic, chloroplastic, and vacuolar compartments and in the phloem sap of spinach leaves. Plant Physiol **97:** 227–233

Sacchi GA, Cocucci M (1992) Effects of deuterium oxide on growth, proton extrusion, potassium influx, and in vitro plasma membrane activities in maize root segments. Plant Physiol **100:** 1962–1967

Saeman JF, Bubl JL, Harris EE (1945) Quantitative saccharification of wood and cellulose. Ind Eng Chem **17:** 35–37

Schaefer J, Skokut TA, Stejskal EO, McKay RA, Varner JE (1981) Estimation of protein turnover in soybean leaves using magic angle double cross-polarization nitrogen 15 nuclear magnetic resonance. J Biol Chem **256:** 11574–11579

Scheible WR, Krapp A, Stitt M (2000) Reciprocal changes of phosphenolpyruvate carboxylase and cytosolic pyruvate kinase, citrate synthase and NADP-isocitrate dehydrogenase expression regulate organic acid metabolism during nitrate assimilation in tobacco leaves. Plant Cell Environ **23:** 1155–1167

Scheurwater I, Dünnebacke M, Eising R, Lambers H (2000) Respiratory costs and rate of protein turnover in the roots of a fast-growing (*Dactylis glomerata* L.) and a slow-growing (*Festuca ovina* L.) grass species. J Exp Bot **51:** 1089–1097

Schütz W, Hausmann N, Krug K, Hampp R, Macek B (2011) Extending SILAC to proteomics of plant cell lines. Plant Cell **23:** 1701–1705

Smith AM, Stitt M (2007) Coordination of carbon supply and plant growth. Plant Cell Environ **30:** 1126–1149

Somerville C, Bauer S, Brininstool G, Facette M, Hamann T, Milne J, Osborne E, Paredez A, Persson S, Raab T, et al (2004) Toward a systems approach to understanding plant cell walls. Science **306:** 2206–2211

Stitt M, Zeeman SC (2012) Starch turnover: pathways, regulation and role in growth. Curr Opin Plant Biol **15:** 282–292

Sulpice R, Flis A, Ivakov AA, Apelt F, Krohn N, Encke B, Abel C, Feil R, Lunn JE, Stitt M (2014) Arabidopsis coordinates the diurnal regulation of carbon allocation and growth across a wide range of photoperiods. Mol Plant **7:** 137–155

Sweetlove LJ, Obata T, Fernie AR (2014) Systems analysis of metabolic phenotypes: what have we learnt? Trends Plant Sci **19:** 222–230

Szecowka M, Heise R, Tohge T, Nunes-Nesi A, Vosloh D, Huege J, Feil R, Lunn J, Nikoloski Z, Stitt M, et al (2013) Metabolic fluxes in an illuminated *Arabidopsis* rosette. Plant Cell **25:** 694–714

Tcherkez G, Boex-Fontvieille E, Mahé A, Hodges M (2012a) Respiratory carbon fluxes in leaves. Curr Opin Plant Biol **15:** 308–314

Tcherkez G, Mahé A, Guérard F, Boex-Fontvieille ER, Gout E, Lamothe M, Barbour MM, Bligny R (2012b) Short-term effects of CO_2 and O_2 on citrate metabolism in illuminated leaves. Plant Cell Environ **35:** 2208–2220

Thimm O, Bläsing O, Gibon Y, Nagel A, Meyer S, Krüger P, Selbig J, Müller LA, Rhee SY, Stitt M (2004) MAPMAN: a user-driven tool to display genomics data sets onto diagrams of metabolic pathways and other biological processes. Plant J **37:** 914–939

Thomson JF (1963) Biological Effects of Deuterium. Pergamon Press, New York, pp 4–5

Tovar-Méndez A, Miernyk JA, Randall DD (2003) Regulation of pyruvate dehydrogenase complex activity in plant cells. Eur J Biochem **270:** 1043–1049

Tschoep H, Gibon Y, Carillo P, Armengaud P, Szecowka M, Nunes-Nesi A, Fernie AR, Koehl K, Stitt M (2009) Adjustment of growth and central metabolism to a mild but sustained nitrogen-limitation in Arabidopsis. Plant Cell Environ **32:** 300–318

Urbanczyk-Wochniak E, Baxter C, Kolbe A, Kopka J, Sweetlove LJ, Fernie AR (2005) Profiling of diurnal patterns of metabolite and transcript abundance in potato (*Solanum tuberosum*) leaves. Planta **221:** 891–903

Usadel B, Bläsing OE, Gibon Y, Höhne M, Günter M, Stitt M (2008) Global transcript levels respond to small changes of the carbon status during progressive exhaustion of carbohydrates in Arabidopsis rosettes. Plant Physiol **146:** 1834–1861

Weiner H, Heldt HW (1992) Inter- and intracellular distribution of amino acids and other metabolites in maize (*Zea mays* L.) leaves. Planta **187:** 242–246

Williams TC, Poolman MG, Howden AJ, Schwarzlander M, Fell DA, Ratcliffe RG, Sweetlove LJ (2010) A genome-scale metabolic model accurately predicts fluxes in central carbon metabolism under stress conditions. Plant Physiol **154:** 311–323

Winter H, Lohaus G, Heldt HW (1992) Phloem transport of amino acids in relation to their cytosolic levels in barley leaves. Plant Physiol **99:** 996–1004

Yang XY, Chen WP, Rendahl AK, Hegeman AD, Gray WM, Cohen JD (2010) Measuring the turnover rates of Arabidopsis proteins using deuterium oxide: an auxin signaling case study. Plant J **63:** 680–695

Yee JC, Jacob NM, Jayapal KP, Kok YJ, Philp R, Griffin TJ, Hu WS (2010) Global assessment of protein turnover in recombinant antibody producing myeloma cells. J Biotechnol **148:** 182–193

Young JD, Shastri AA, Stephanopoulos G, Morgan JA (2011) Mapping photoautotrophic metabolism with isotopically nonstationary ^{13}C flux analysis. Metab Eng **13:** 656–665

Yuan J, Bennett BD, Rabinowitz JD (2008) Kinetic flux profiling for quantitation of cellular metabolic fluxes. Nat Protoc **3:** 1328–1340

Yuan J, Fowler WU, Kimball E, Lu W, Rabinowitz JD (2006) Kinetic flux profiling of nitrogen assimilation in Escherichia coli. Nat Chem Biol **2:** 529–530

Zhou H, Li W, Wang SP, Mendoza V, Rosa R, Hubert J, Herath K, McLaughlin T, Rohm RJ, Lassman ME, et al (2012) Quantifying apoprotein synthesis in rodents: coupling LC-MS/MS analyses with the administration of labeled water. J Lipid Res **53:** 1223–1231